

# Pentacoordinate Anionic Bis(siliconates) Containing a Fluorine Bridge between Two Silicon Atoms. Synthesis, Solid-State Structures, and Dynamic Behavior in Solution

Kohei Tamao,\* Takashi Hayashi, and Yoshihiko Ito\*

Department of Synthetic Chemistry, Faculty of Engineering, Kyoto University, Kyoto 606, Japan

Motoo Shiro

Shionogi Research Laboratory, Fukushima-ku, Osaka 553, Japan

Received January 29, 1992

The pentacoordinate anionic bis(siliconates)  $[o\text{-C}_6\text{H}_4(\text{SiPhF}_2)_2\text{F}]^-\text{K}^+\cdot 18\text{-crown-6}$  (1),  $[o\text{-C}_6\text{H}_4(\text{SiF}_3)(\text{SiPh}_2\text{F})\text{F}]^-\text{K}^+\cdot 18\text{-crown-6}$  (2), and  $[o\text{-C}_6\text{H}_4(\text{SiPhF}_2)(\text{SiPh}_2\text{F})\text{F}]^-\text{K}^+\cdot 18\text{-crown-6}$  (3) have been prepared from the corresponding *o*-disilylbenzene derivatives, by treatment with KF and 18-crown-6 in toluene at room temperature, as stable white crystals. The X-ray crystallography of 1-3 confirms the presence of a bent, unsymmetrical fluoride bridge between two silicon atoms. The geometry about each silicon atom is a deformed trigonal bipyramid (TBP) with two fluorine atoms occupying the apical positions and with the silicon atom being displaced slightly out of the equatorial plane, indicating residual tetrahedral character; the deviation depends on the number of fluorine ligands on the silicon atom. The apical Si-F bond lengths are correlated with pentacoordination characters,  $\text{TBP}_a$  and  $\text{TBP}_e$ , defined by apical-to-equatorial and equatorial-to-equatorial bond angles, respectively. The results suggest that bis(siliconates) 1-3 can be regarded as the sequential models for the structural change from tetrahedral silane to pentacoordinate (TBP) siliconate in nucleophilic attack on a silicon atom.  $^{13}\text{C}$ ,  $^{19}\text{F}$ , and  $^{29}\text{Si}$  NMR spectra of three bis(siliconates) have been examined to elucidate the solution structures. A solid-state MAS  $^{29}\text{Si}$  NMR study has also been conducted for the first time on 2 and on the mono(siliconate)  $[\text{PhSiF}_4]^-$  to correlate with the solution structures. At room temperature or above,  $^{19}\text{F}$  NMR spectra for 1 and 3 show a broad singlet each for all fluorine atoms owing to fast intramolecular exchange on the  $^{19}\text{F}$  NMR time scale, while five fluorine atoms in 2 appear as two sharp singlets in the ratio of 4:1. The  $^{29}\text{Si}$  NMR signal for 1 appears as a sextet due to coupling with five equivalent fluorine atoms at room temperature.  $^{13}\text{C}$  NMR spectra for the ipso and ortho positions of 1 and 3 also exhibit sextets and quintets due to coupling with five and four equivalent fluorine atoms, respectively. These NMR studies demonstrate that 1 and 3 are the first examples of anionic siliconates in which all fluorine ligands undergo fast exchange over two silicon atoms. At the low-temperature limits,  $^{19}\text{F}$  NMR spectra for 1-3 show ground-state structures:  $\text{F}_{\text{br}}$ ,  $\text{F}_{\text{ap}}$ , and  $\text{F}_{\text{eq}}$  atoms appear as individual signals. The dynamic variable-temperature  $^{19}\text{F}$  NMR spectra have been interpreted by the following consecutive processes for intramolecular ligand exchange: (a) exchange of  $\text{F}_{\text{br}}$  between tetraordinate and pentacoordinate silicon atoms, (b) flipping of the  $\text{F}_{\text{br}}$ -containing five-membered ring, (c) full rotation about the Si-C bond, and (d) pseudorotation at pentacoordinate silicon centers. The ease of these processes is correlated well with the pentacoordination character, % TBP, of silicon atoms estimated from the solid-state structures.

## Introduction

Penta- and hexacoordinate silicon compounds have recently attracted a great deal of interest from structural and mechanistic points of view.<sup>1</sup> In particular, pentacoordinate anionic siliconates have long been recognized as the reaction intermediates in nucleophilic substitution at silicon atoms.<sup>2</sup> The geometry of pentacoordinate anionic siliconate was first confirmed by Schomburg in 1981, who performed an X-ray structure analysis of  $[\text{PhSiF}_4][n\text{-Pr}_4\text{N}]$  in which the geometry about the silicon atom was trigonal bipyramidal (TBP) with two fluorine atoms preferentially occupying the apical positions.<sup>3</sup> After the presentation of Schomburg's work, a great deal of reports have dealt

with structures and fundamental aspects of stability of anionic pentacoordinate *mono(siliconates)*, which contain only one silicon atom in a molecule. Damrauer and his co-workers first reported nonhygroscopic fluorosiliconates as the  $\text{K}^+\cdot 18\text{-crown-6}$  salts.<sup>4a</sup> Subsequently, Holmes and his co-workers have reported the isolation and structural analysis of a series of  $[\text{R}_n\text{SiF}_{5-n}]^-$  species,<sup>5,6</sup> especially sterically crowded fluorosiliconates such as  $[\text{Mes}_2\text{SiF}_3]^-$ <sup>6a</sup> and  $[(\text{TTBP})\text{SiF}_4]^-$ ,<sup>6b</sup> where Mes and TTBP stand for the mesityl and 2,4,6-tri-*tert*-butylphenyl groups, respectively. These studies have demonstrated that the bond parameters around the silicon atom highly depend on the steric hindrance of organic groups R and on the number of fluorine ligands.<sup>5</sup> A number of pentacoordinate mono(siliconates) containing anionic chelate ligands such as catecholate, pinacolate, and Martin ligands<sup>7</sup> have also been studied, which involve the first examples of cyano-

(1) (a) Corriu, R. J. P.; Young, J. C. In *The Chemistry of Organic Silicon Compounds*; Patai, S., Rappoport, Z., Eds.; Wiley: Chichester, U.K., 1989; Part 2, Chapter 20. (b) Tandura, St. N.; Alekseev, N. V.; Voronkov, M. G. *Top. Curr. Chem.* 1986, 131, 99-189.

(2) (a) Holmes, R. R. *Chem. Rev.* 1990, 90, 17. (b) Corriu, R. J. P. *J. Organomet. Chem.* 1990, 400, 81. (c) Corriu, R. J. P.; Guerin, C.; Moreau, J. J. E. In *The Chemistry of Organic Silicon Compounds*; Patai, S., Rappoport, Z., Eds.; Wiley: Chichester, U.K., 1989; Part 1, Chapter 4. (d) Bassindale, A. R.; Taylor, P. G. In *The Chemistry of Organic Silicon Compounds*; Patai, S., Rappoport, Z., Eds.; Wiley: Chichester, U.K., 1989; Part 1, Chapter 13. (e) Gordon, M. S.; Davis, L. P.; Burggraf, L. W.; Damrauer, R. *J. Am. Chem. Soc.* 1986, 108, 7889. (f) Damrauer, R.; Burggraf, L. W.; Davis, L. P.; Gordon, M. S. *J. Am. Chem. Soc.* 1988, 110, 6601. (g) Deiters, J. A.; Holmes, R. R. *J. Am. Chem. Soc.* 1987, 109, 1686, 1692. (h) DePuy, C. E.; Damrauer, R.; Bowie, J. H.; Sheldon, J. C. *Acc. Chem. Res.* 1987, 20, 127.

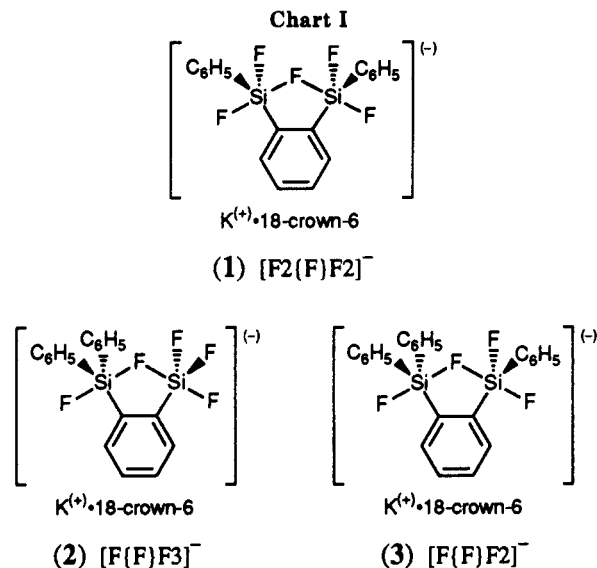
(3) Schomburg, D. *J. Organomet. Chem.* 1981, 221, 137.

(4) (a) Damrauer, R.; Danahey, S. E. *Organometallics* 1986, 5, 1490. (b) Damrauer, R.; O'Connell, B.; Danahey, S. E.; Simon, R. *Organometallics* 1989, 8, 1167.

(5) Harland, J. J.; Payne, J. S.; Day, R. O.; Holmes, R. R. *Inorg. Chem.* 1987, 26, 760.

(6) (a) Johnson, S. E.; Deiters, J. A.; Day, R. O.; Holmes, R. R. *J. Am. Chem. Soc.* 1989, 111, 3250. (b) Johnson, S. E.; Day, R. O.; Holmes, R. R. *Inorg. Chem.* 1989, 28, 3182. (c) Johnson, S. E.; Payne, J. S.; Day, R. O.; Holmes, J. M.; Holmes, R. R. *Inorg. Chem.* 1989, 28, 3190.

(7) (a) Stevenson, W. H. III; Wilson, S.; Martin, J. C.; Farnham, W. B. *J. Am. Chem. Soc.* 1985, 107, 6340. (b) Stevenson, W. H., III; Martin, J. C. *J. Am. Chem. Soc.* 1985, 107, 6352.



siliconates,<sup>8</sup> silylsiliconates,<sup>9</sup> and pentaalkoxysiliconates.<sup>10</sup>

In contrast, for *bis(siliconates)*, which contain two pentacoordinate silicon atoms in a molecule, only one example,  $[F_4SiCH_2CH_2SiF_4]^{2-}[K^+ \cdot 18\text{-crown-6}]_2$ ,<sup>6b</sup> has recently been reported. This *bis(siliconate)*, however, appears to contain no fluorine bridge between the two silicon atoms. Two works may be mentioned in this connection. Janzen and his co-workers examined intermolecular fluoride-exchange phenomena between tetracoordinate fluorosilanes and pentacoordinate methyl- or phenyltetrafluorosilicate by <sup>19</sup>F NMR measurements, suggesting the presence of the fluorine-bridged siliconate dimer  $[RF_3Si-F-SiF_3R]^-$  in solution.<sup>11</sup> Brownstein also reported the observation of the linear F-bridged species  $[(AcO)F_3Si-F-SiF_3(OAc)]^-$  in solution by NMR measurements.<sup>12</sup>

In a preliminary report,<sup>13</sup> we presented the first example of a *bis(siliconate)* containing an Si-F-Si bond,  $[o\text{-C}_6\text{H}_4\text{(SiPhF}_2)_2\text{F}]^-[K^+ \cdot 18\text{-crown-6}]$  (1). This report describes the full details of the solid-state structures of 1 and the unsymmetrical analogues  $[o\text{-C}_6\text{H}_4\text{(SiF}_3\text{(SiPh}_2\text{F)F)]}^-[K^+ \cdot 18\text{-crown-6}]$  (2) and  $[o\text{-C}_6\text{H}_4\text{(SiPhF}_2\text{(SiPh}_2\text{F)F)]}^-[K^+ \cdot 18\text{-crown-6}]$  (3) (Chart I). For clarity, throughout this paper, these *bis(siliconates)* 1-3 may be abbreviated  $[F_2(F)F_2]^-$ ,  $[F(F)F_3]^-$ , and  $[F(F)F_2]^-$ , respectively, in which the central [F] represents the bridging fluorine atom and the left and right sides represent the number of fluorine atoms on the two silicon atoms.

An X-ray structural analysis of the three *bis(siliconates)* has afforded new significant information about bond lengths and bond angles. It has thus been found that there are linear relationships between the Si-F and Si-C bond lengths and the pentacoordination character of the silicon atoms defined by bond angles. Thus, the structures of these *bis(siliconates)* provide visual, sequential models for nucleophilic attack on a tetrahedral (TH) silicon center approaching a pentacoordinate TBP siliconate complex.

<sup>13</sup>C, <sup>19</sup>F, and <sup>29</sup>Si NMR spectra of 1-3 in solution have shown that these compounds are the first examples where

(8) Dixon, D. A.; Hertler, W. R.; Chase, D. B.; Farnham, W. B.; Davidson, F. *Inorg. Chem.* 1988, 27, 4012.

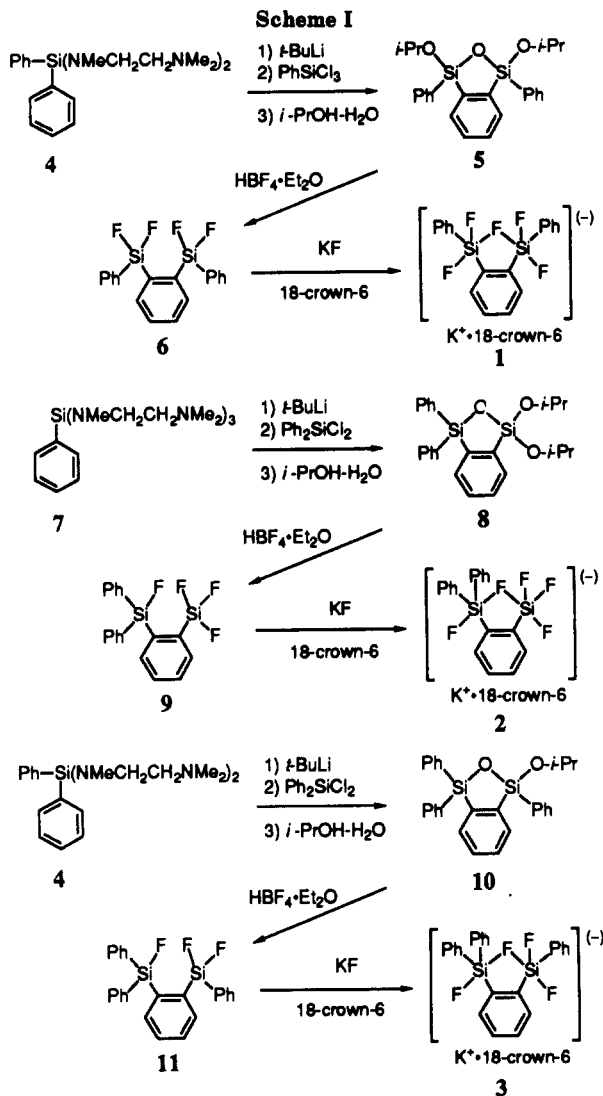
(9) Kira, M.; Sato, K.; Kabuto, C.; Sakurai, H. *J. Am. Chem. Soc.* 1989, 111, 3747.

(10) Kumara Swamy, K. C.; Chandrasekhar, V.; Harland, J. J.; Holmes, J. M.; Day, R. O.; Holmes, R. R. *J. Am. Chem. Soc.* 1990, 112, 2341.

(11) Marat, R. K.; Janzen, A. F. *Can. J. Chem.* 1977, 55, 1167, 3845.

(12) Brownstein, S. *Can. J. Chem.* 1980, 58, 1407.

(13) Tamao, K.; Hayashi, T.; Ito, Y.; Shiro, M. *J. Am. Chem. Soc.* 1990, 112, 2422.



four or five fluorine atoms undergo intramolecular exchange over two silicon atoms. Solid-state MAS <sup>29</sup>Si NMR spectra for mono- and *bis(siliconates)* are also represented for the first time. Mechanisms for the fluorine ligand exchange will be discussed in terms of consecutive multistep processes based on variable-temperature <sup>19</sup>F NMR spectra: Three new mechanisms, in addition to the pseudorotation, will be introduced. We will attempt to correlate the dynamic behavior in solution with the pentacoordination characters of silicon atoms estimated from the solid-state structures.

## Results and Discussion

**I. Synthesis.** The synthetic routes to the anionic *bis(siliconates)* 1-3 are shown in Scheme I. The precursor *o*-disilylbenzenes were prepared by selective ortho lithiation directed by amino groups on silicon.<sup>14</sup> The ortho-lithiated species of bis(trimethylethylenediamino)di-phenylsilane (4) was quenched with PhSiCl<sub>3</sub>, followed by alcoholysis with 2-propanol to give the cyclic *o*-disilylbenzene derivative 5 in 57% yield. Fluorination of 5 by a tetrafluoroboric acid-diethyl ether complex proceeded smoothly to give *o*-bis(difluorophenylsilyl)benzene (6) in quantitative yield. Treatment of 6 with 1 equiv of spray-dried KF and 18-crown-6 in toluene at room tem-

(14) Tamao, K.; Yao, H.; Tsutsumi, Y.; Abe, H.; Hayashi, T.; Ito, Y. *Tetrahedron Lett.* 1990, 31, 2925.

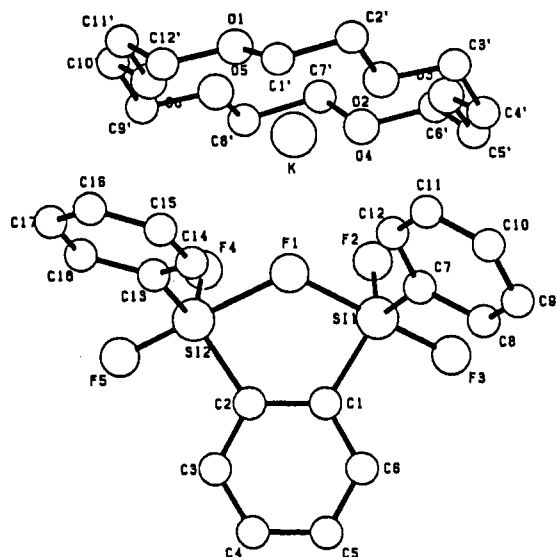
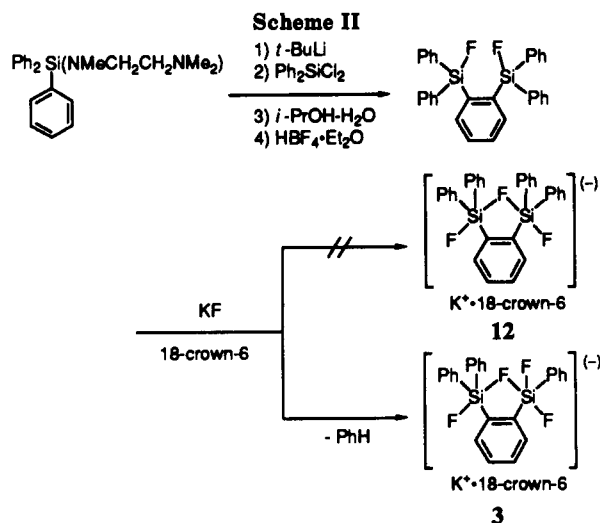


**Figure 1.** X-ray crystal structure of  $[o\text{-C}_6\text{H}_4(\text{SiPhF}_2)_2\text{F}]^-, \text{K}^+$ , 18-crown-6 (1).

perature for 20 h, according to the Damrauer method,<sup>4a</sup> gave a white crystalline solid which was recrystallized from dry THF to give pure 1 in 64% yield. Bis(silicate) 1 is air-stable but slightly hygroscopic and decomposes at 149.5–150.5 °C. Bis(silicates) 2 and 3 were prepared similarly. Thus, tris(trimethylethylenediamino)phenylsilane (7) and 4 were lithiated and quenched with Ph<sub>2</sub>SiCl<sub>2</sub> to give the corresponding *o*-disilylbenzene derivatives 8 and 10, respectively. Preparations of the anionic siliconates 2 and 3 from 8 and 10, respectively, were accomplished in the same manner as above. Bis(silicates) 2 and 3 are also air-stable and are less hygroscopic than 1. All three siliconates were characterized by <sup>1</sup>H, <sup>13</sup>C, and <sup>19</sup>F NMR spectroscopy and elemental analysis.

Attempted preparation of the symmetrical bis(silicate) [F{F}F]<sup>-</sup>,  $[o\text{-C}_6\text{H}_4(\text{SiPh}_2\text{F})_2\text{F}]^-, \text{K}^+$ ·18-crown-6 (12), failed. Thus, treatment of *o*-bis(fluorodiphenylsilyl)benzene, prepared similarly, with KF did not give the expected product 12 but gave bis(silicate)  $[\text{F}\{\text{F}\}\text{F}_2]^-$  (3) via cleavage of one Si–phenyl bond, as shown in Scheme II. In an attempted preparation of the dianionic bis(silicate)  $[o\text{-C}_6\text{H}_4(\text{SiPhF}_3)_2]^{2-}$ , which might be formed by inclusion of two fluoride ions, fluorosilane 6 was allowed to react with more than 2 equiv of KF, but only a mixture of bis(silicate) 1 and uncharacterizable product (1:2 by <sup>1</sup>H NMR measurements) was obtained.

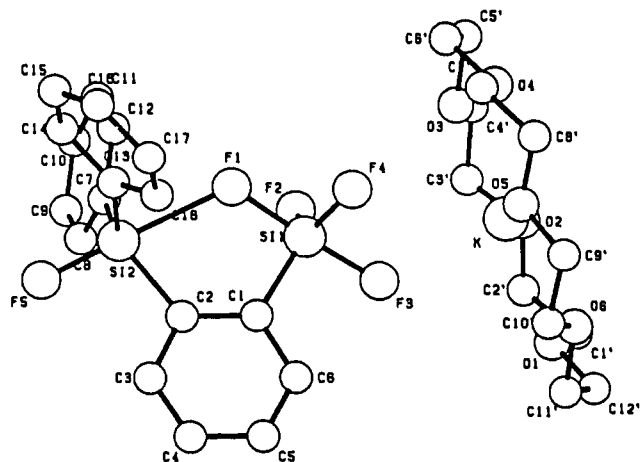


**Figure 2.** X-ray crystal structure of  $[o\text{-C}_6\text{H}_4(\text{SiF}_3)(\text{SiPh}_2\text{F})\text{-F}]^-, \text{K}^+$ ·18-crown-6 (2).

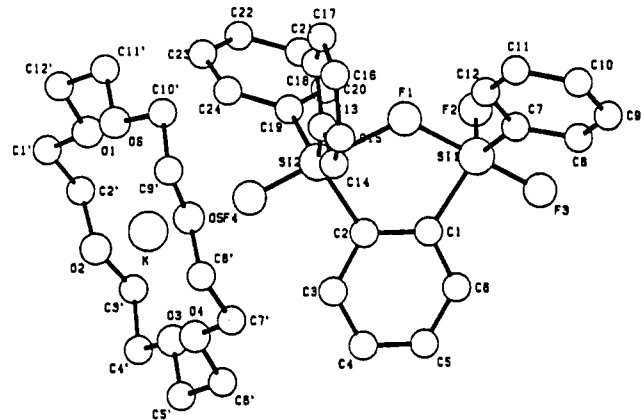


**Figure 3.** X-ray crystal structure of  $[o\text{-C}_6\text{H}_4(\text{SiPhF}_2)(\text{SiPh}_2\text{F})\text{-F}]^-, \text{K}^+$ ·18-crown-6 (3).

**Table I.** Selected Bond Lengths (Å) and Angles (deg) for  $[o\text{-C}_6\text{H}_4(\text{SiPhF}_2)_2\text{F}][\text{K}^+ \cdot 18\text{-crown-6}]$  (1)<sup>a</sup>

Distances			
Si1–F1	1.898 (4)	Si2–F1	2.065 (4)
Si1–F2	1.616 (4)	Si2–F4	1.601 (4)
Si1–F3	1.657 (4)	Si2–F5	1.638 (4)
Si1–C1	1.877 (5)	Si2–C2	1.867 (2)
Si1–C7	1.879 (5)	Si2–C13	1.871 (5)
K–F1	3.042 (3)	K–F4	3.073 (3)
K–F2	2.780 (3)		
Angles			
F1–Si1–F2	82.3 (2)	F1–Si2–F4	80.9 (2)
F1–Si1–F3	172.6 (2)	F1–Si2–F5	174.5 (2)
F1–Si1–C1	85.0 (2)	F1–Si2–C2	81.7 (2)
F1–Si1–C7	90.4 (2)	F1–Si2–C13	87.4 (2)
F2–Si1–F3	91.4 (2)	F4–Si2–F5	94.6 (2)
F2–Si1–C1	124.0 (2)	F4–Si2–C2	119.1 (2)
F2–Si1–C7	117.7 (2)	F4–Si2–C13	115.6 (2)
F3–Si1–C1	95.3 (2)	F5–Si2–C2	97.9 (2)
F3–Si1–C7	96.1 (2)	F5–Si2–C13	97.4 (2)
C1–Si1–C7	116.7 (2)	C2–Si2–C13	121.3 (2)
Si1–F1–Si2	119.7 (2)		

<sup>a</sup> Estimated standard deviations are given in parentheses. The atom-labeling scheme is shown in Figure 1.

**II. Solid-State Structures of X-ray Crystallography.** X-ray structural studies were conducted on bis(silicates) 1–3. The structures are shown in Figures 1–3. Selected bond lengths and angles are listed in Tables I–III, while a summary of the crystallographic data, intensity collection, and least-squares processing is shown in Table IV. Atomic coordinates and equivalent isotropic temperature factors are provided as supplementary material.

**Table II. Selected Bond Lengths (Å) and Angles (deg) for [*o*-C<sub>6</sub>H<sub>4</sub>(SiF<sub>3</sub>)(SiPh<sub>2</sub>F)]K•18-crown-6 (2)<sup>a</sup>**

Distances			
Si1-F1	1.700 (3)	Si2-F1	2.369 (3)
Si1-F2	1.598 (4)	Si2-F5	1.639 (3)
Si1-F3	1.667 (4)	Si2-C2	1.872 (4)
Si1-F4	1.615 (4)	Si2-C7	1.870 (4)
Si1-C1	1.880 (4)	Si2-C13	1.878 (4)
K-F3	2.720 (4)	K-F4	3.027 (4)
K-F5'	2.724 (2)		
Angles			
F1-Si1-F2	88.0 (2)	F1-Si2-C7	82.0 (1)
F1-Si1-F3	176.2 (2)	F1-Si2-F5	178.4 (1)
F1-Si1-F4	88.4 (2)	F1-Si2-C13	80.8 (1)
F1-Si1-C1	89.5 (1)	F1-Si2-C2	78.3 (1)
F2-Si1-F3	90.5 (2)	F5-Si2-C7	98.1 (1)
F2-Si1-F4	116.3 (2)	C7-Si2-C13	117.1 (2)
F2-Si1-C1	121.8 (2)	C2-Si2-C7	121.5 (2)
F3-Si1-F4	89.1 (2)	F5-Si2-C13	100.6 (2)
F3-Si1-C1	94.3 (2)	F5-Si2-C2	100.4 (1)
F4-Si1-C1	121.7 (2)	C2-Si2-C13	113.1 (2)
Si1-F1-Si2	118.6 (1)		

<sup>a</sup> Estimated standard deviations are given in parentheses. The atom-labeling scheme is shown in Figure 2.

**Table III. Selected Bond Lengths (Å) and Angles (deg) for [*o*-C<sub>6</sub>H<sub>4</sub>(SiPhF<sub>2</sub>)(SiPh<sub>2</sub>F)]K•18-crown-6 (3)<sup>a</sup>**

Distances			
Si1-F1	1.805 (2)	Si2-F1	2.090 (2)
Si1-F2	1.624 (3)	Si2-F4	1.672 (3)
Si1-F3	1.669 (3)	Si2-C2	1.876 (4)
Si1-C1	1.896 (4)	Si2-C13	1.860 (4)
Si1-C7	1.889 (4)	Si2-C19	1.887 (4)
K-F4	2.639 (3)		
Angles			
F1-Si1-F2	85.2 (1)	F1-Si2-F4	177.5 (1)
F1-Si1-F3	174.6 (1)	F1-Si2-C2	81.7 (1)
F1-Si1-C1	86.3 (1)	F1-Si2-C13	82.7 (1)
F1-Si1-C7	90.9 (1)	F1-Si2-C19	86.7 (1)
F2-Si1-F3	90.0 (1)	F4-Si2-C2	97.6 (1)
F2-Si1-C1	118.5 (1)	F4-Si2-C13	95.7 (1)
F2-Si1-C7	115.9 (1)	F4-Si2-C19	95.7 (1)
F3-Si1-C1	93.9 (1)	C2-Si2-C13	121.1 (2)
F3-Si1-C7	93.4 (1)	C2-Si2-C19	118.6 (2)
C1-Si1-C7	125.0 (2)	C13-Si2-C19	116.6 (2)
Si1-F1-Si2	126.1 (1)		

<sup>a</sup> Estimated standard deviations are given in parentheses. The atom-labeling scheme is shown in Figure 3.

While the atom-labeling schemes are shown in Figures 1-3, the abbreviations F<sub>br</sub>, F<sub>ap</sub>, F<sub>eq</sub>, and C<sub>eq</sub> are used for the bridging F, apical F, equatorial F, and equatorial C atoms, respectively.

Compounds 1-3 represent the first anionic fluoro-siliconates containing a bent fluorine bridge between two silicon atoms. Si1-F1<sub>br</sub>-Si2 angles in 1-3 are 118.6, 119.7, and 126.0°, respectively. In all three compounds, the fluorine bridge is unsymmetrical with different bond lengths for F1<sub>br</sub>-Si1 and F1<sub>br</sub>-Si2, as will be discussed later. The geometries about the silicon atoms are deformed TBP with two electronegative fluorine atoms occupying the apical positions. For example, in [F2{F}F2]<sup>-</sup> (1), F1 and F3 occupy the apical positions and C1-F2-C7 constitutes the equatorial plane on the Si1 side, while the apical fluorines and the equatorial plane on the Si2 side are F1 and F5 and C2-F4-C13. The molecular distortion modes observed in 1-3, however, differ from those observed in pentacoordinate mono(siliconates) thus far reported, as will be discussed later. In alternative descriptions, bis(siliconates) 1-3 consist of two diaryltrifluorosilicate [Ar<sub>2</sub>SiF<sub>3</sub>]<sup>-</sup> moieties, one [ArSiF<sub>4</sub>]<sup>-</sup> and one [Ar<sub>3</sub>SiF<sub>2</sub>]<sup>-</sup> moiety, and one [Ar<sub>2</sub>SiF<sub>3</sub>]<sup>-</sup> and one [Ar<sub>3</sub>SiF<sub>2</sub>]<sup>-</sup> moiety, respectively, sharing one apical fluorine (F1<sub>br</sub>) in each case.

**Thermal Motions of the Bridging Fluoride.** In our previous communication, we have presented the molecular structure of 1 drawn with thermal ellipsoids.<sup>13</sup> The structure demonstrates that the ellipsoid of the bridging fluorine F1<sub>br</sub> is small and has a nearly regular ball shape. Anisotropic thermal parameters of F1<sub>br</sub> are roughly equal to each other ( $U_{11} = [55 (1)] \times 10^3$ ,  $U_{22} = [50 (1)] \times 10^3$ , and  $U_{33} = [41 (1)] \times 10^3 \text{ Å}^2$ ). Thus, thermal motion of F1<sub>br</sub> between Si1 and Si2 is not large in the crystal. Also in the case of 2 and 3, there is no large thermal motion of F1<sub>br</sub>. These parameters for all three compounds are provided as supplementary material.

**F<sub>br</sub>-Containing Five-Membered Ring.** While the F<sub>br</sub>-containing five-membered rings in 1 and 2 are puckered, 3 contains a nearly planar five-membered ring. Thus, the angle between the Si1-C1<sub>eq</sub>-C2<sub>eq</sub>-Si2 plane and the Si1-F1<sub>br</sub>-Si2 plane in 1-3 is 34.0 (2)<sup>o</sup>, 26.5 (2)<sup>o</sup>, and 0.2 (1)<sup>o</sup>, respectively.

The puckering is correlated with the dihedral angle between the equatorial plane and the core benzene ring, C1-C6. The dihedral angles between these planes in 1 are

**Table IV. Summary of Crystal Data, Intensity Collection, and Least-Squares Processing for 1-3**

	1	2	3
formula	C <sub>30</sub> H <sub>38</sub> O <sub>6</sub> F <sub>5</sub> Si <sub>2</sub> K	C <sub>30</sub> H <sub>38</sub> O <sub>6</sub> F <sub>5</sub> Si <sub>2</sub> K	C <sub>36</sub> H <sub>48</sub> O <sub>6</sub> F <sub>4</sub> Si <sub>2</sub> K
fw	684.9	684.9	743.0
cryst syst	triclinic	monoclinic	orthorhombic
space group	P1	P2 <sub>1</sub>	Pbca
a, Å	10.702 (3)	11.368 (1)	16.810 (1)
b, Å	11.158 (4)	16.632 (1)	25.667 (1)
c, Å	8.500 (3)	9.793 (1)	17.191 (1)
α, deg	113.79 (3)		
β, deg	108.02 (2)	115.67 (1)	
γ, deg	64.89 (3)		
V, Å <sup>3</sup>	829.2 (5)	1668.8 (3)	7417.2 (8)
Z	1	2	8
ρ <sub>calcd</sub> , g cm <sup>-3</sup>	1.372	1.363	1.331
μ(Cu Kα), cm <sup>-1</sup>	26.7	26.5	23.9
cryst size, mm	0.50 × 0.40 × 0.10	0.30 × 0.30 × 0.15	0.35 × 0.35 × 0.35
2θ <sub>max</sub> , deg	120	120	110
total no. of unique rflns	2462	2573	3736
no. of obsd rflns with F <sub>o</sub> > 3σ(F <sub>o</sub> )	2366	2547	3409
no. of rflns with w <sup>1/2</sup>  ΔF  < 4 used at the last stage of refinement	2356	2524	3298
no. of params refined	508	510	571
R	0.034	0.032	0.039
R <sub>w</sub>	0.047	0.045	0.061
S	1.081	1.087	1.338

71.6 (2)° on the Si1 side and 66.1 (2)° on the Si2 side (cf. Scheme IVb, mentioned later). In bis(siliconate) 2, these angles are 72.3 (1) and 80.6 (1)°. In contrast, 3 has a dihedral angle of 89.5 (1)° on both sides, indicating that the two equatorial planes lie nearly perpendicular to the benzene ring. Thus, the puckering is caused by partial rotation about the C1-Si1 and C2-Si2 bonds involved in the equatorial planes. Although the reason for the conformational difference is not clear yet, these results clearly indicate that the F<sub>br</sub>-containing five-membered ring can be puckered or planar.

**Stereochemistry.** There would be two possible stereoisomers, *cis* and *trans*, in 1, but only the *cis* isomer has been found. The main reason may reside in the interaction between the counteraction K<sup>+</sup> and the three fluorine atoms F1<sub>br</sub>, F2<sub>eq</sub>, and F4<sub>eq</sub>, as discussed below.

**K<sup>+</sup>-F Interaction.** It is of interest to compare the position of the potassium ion as the counteraction: completely different modes of K<sup>+</sup>-F interaction in 1-3 may be noted. For reference, the shortest and the longest K-F distances found in a series of [R<sub>n</sub>SiF<sub>5-n</sub>]<sup>-</sup>K<sup>+</sup>-18-crown-6 species are 2.544 (4) and 3.037 (4) Å, respectively, in [t-BuPhSiF<sub>3</sub>]<sup>-</sup>.<sup>6c</sup> In a series of [(p-XC<sub>6</sub>H<sub>4</sub>)PhSiF<sub>3</sub>]<sup>-</sup>K<sup>+</sup>-18-crown-6 compounds which involve no steric deformation, the average K-F distance is 2.875 Å for K-F<sub>ap</sub> and 2.629 Å for K-F<sub>eq</sub>.<sup>15</sup> The K-F distance in potassium fluoride is 2.67 Å.<sup>16</sup>

**[F<sub>2</sub>(F)F<sub>2</sub>]<sup>-</sup> (1).** The K<sup>+</sup> ion interacts with the three fluorine atoms F1<sub>br</sub>, F2<sub>eq</sub>, and F4<sub>eq</sub>. Significantly, K<sup>+</sup> is in close proximity to one equatorial F2, K-F2<sub>eq</sub> = 2.780 (3) Å, rather than to the apical F1, K-F1<sub>br</sub> = 3.042 (3) Å (and to the other equatorial fluorine, F4, K-F4<sub>eq</sub> = 3.073 (3) Å). This feature is in contrast to the case for most of the known fluoro mono(siliconates), where the K<sup>+</sup> ion interacts with two fluorine atoms, with a shorter distance to the apical than to the equatorial fluorine.<sup>5,6</sup> It should be further noted that even the shortest K-F2<sub>eq</sub> distance in 1 seems to be longer than the short K-F<sub>eq</sub> distances ever found in fluoro mono(siliconate), demonstrating looser K-F interaction in the present case.<sup>16</sup>

**[F(F)F<sub>3</sub>]<sup>-</sup> (2).** The K<sup>+</sup> ion is associated with one apical F3, K-F3<sub>ap</sub> = 2.720 (4) Å, and one equatorial F4, K-F4<sub>eq</sub> = 3.027 (4) Å, on Si1. Interestingly, the K<sup>+</sup> ion is also in contact with one apical F5'<sub>ap</sub> atom in another anion, K-F5'<sub>ap</sub> = 2.724 (2) Å. Thus, the K<sup>+</sup> ion is located between the apical F3 and the apical F5', forming a cation-anion chain. A similar cation-anion chain has been found recently in the mono(siliconate) [MesSiF<sub>4</sub>]<sup>-</sup>K<sup>+</sup>-18-crown-6.<sup>6b</sup>

**[F(F)F<sub>2</sub>]<sup>-</sup> (3).** The K<sup>+</sup> ion is close to only one apical fluorine F4, K-F4<sub>ap</sub> = 2.639 (3) Å, which is the shortest of the K-F<sub>ap</sub> bonds in all three bis(siliconates) and comparable to the K-F distance in potassium fluoride.

**Si-F Bond Lengths.** Selected bond lengths are summarized in Table V. Bis(siliconates) 1-3 contain unusually long and short Si-F<sub>ap</sub> bonds in comparison with those of mono(siliconates) isolated so far. For reference, in a series of [R<sub>n</sub>SiF<sub>5-n</sub>]<sup>-</sup> compounds, Si-F<sub>ap</sub> bond lengths are in the range of 1.646 (1) Å in [SiF<sub>5</sub>]<sup>-</sup><sup>17</sup> to 1.729 (6) Å in [Mes<sub>2</sub>SiF<sub>3</sub>]<sup>-</sup>.<sup>6a</sup>

**[F<sub>2</sub>(F)F<sub>2</sub>]<sup>-</sup> (1).** The endocyclic F1<sub>br</sub>-Si1 and F1<sub>br</sub>-Si2 bond lengths are 1.898 (4) and 2.065 (4) Å, respectively. Thus, the fluorine bridge is unsymmetrical, despite the fact that the parent molecule is symmetrical. It should

Table V. Bond Lengths, Angles (θ<sub>n</sub> and φ<sub>n</sub>), and Deviations (Δ<sub>Si</sub>) in Bis(siliconates) 1-3<sup>a</sup>

	anion of 1		anion of 2		anion of 3	
position	Si2	Si1	Si2	Si1	Si2	Si1
Si-F <sub>ap</sub> , Å						
R <sup>b</sup>	2.065	1.898	2.369	1.700	2.090	1.805
r <sup>b</sup>	1.638	1.657	1.639	1.667	1.672	1.669
Si-F <sub>eq</sub> , Å	1.601	1.616		1.598	1.615	1.624
Si-C <sub>eq</sub> , Å <sup>c</sup>	1.871	1.879	1.870		1.860	1.889
			1.878		1.887	
Δ <sub>Si</sub> , Å <sup>d</sup>	0.205	0.131	0.314	0.040	0.207	0.078
θ <sub>n</sub> (av), deg <sup>e</sup>	96.6	94.3	99.7	91.3	96.3	92.4
φ <sub>n</sub> (av), deg <sup>f</sup>	118.7	119.5	117.2	119.9	118.8	119.8
% TBP <sup>g</sup>	66	78	50	93	68	88
% TBP <sup>h</sup>	88	95	73	99	88	98

<sup>a</sup>The counteraction is K<sup>+</sup>-18-crown-6. <sup>b</sup>R and r denote respectively the Si-F<sub>br</sub> and Si-F<sub>ap</sub> bond lengths, as defined in Scheme III. <sup>c</sup>Exocyclic Si-C<sub>eq</sub> bond lengths. <sup>d</sup>The deviation of the silicon atom out of the equatorial plane. <sup>e</sup>The average of three exocyclic apical-to-equatorial angles, as defined in Scheme III. <sup>f</sup>The average of three equatorial-to-equatorial angles, as defined in Scheme III. <sup>g</sup>Pentacoordination character calculated from θ<sub>n</sub> by eq 1 in the text. <sup>h</sup>Pentacoordination character calculated from φ<sub>n</sub> by eq 2 in the text.

be noted that these apical Si-F bonds are among the longest ones ever found in diorganotrifluorosiliconates [Ar<sub>2</sub>SiF<sub>3</sub>]<sup>-</sup>. On the other hand, the exocyclic Si-F<sub>ap</sub> bonds, Si1-F3<sub>ap</sub> = 1.657 (4) Å and Si2-F5<sub>ap</sub> = 1.638 (4) Å, are among the shortest ones ever found for apical Si-F bonds in the [R<sub>n</sub>SiF<sub>5-n</sub>]<sup>-</sup> series.

**[F(F)F<sub>3</sub>]<sup>-</sup> (2).** Si1-F1<sub>br</sub> and Si2-F1<sub>br</sub> bond lengths are 1.700 (3) and 2.369 (3) Å, respectively. The bridging fluorine F1 is much closer to the highly fluorinated Si1. The Si2-F1<sub>br</sub> bond is the longest Si-F<sub>ap</sub> bond in pentacoordinate fluorosiliconates observed so far, while the other exocyclic apical bond length, Si2-F5<sub>ap</sub> = 1.639 (3) Å, is almost the same as that in 1 and is among the shortest of the known Si-F<sub>ap</sub> bonds in the [R<sub>n</sub>SiF<sub>5-n</sub>]<sup>-</sup> series.

**[F(F)F<sub>2</sub>]<sup>-</sup> (3).** Si1-F1<sub>br</sub> and Si2-F1<sub>br</sub> bond lengths are 1.805 (2) and 2.090 (2) Å, respectively. The Si1-F<sub>br</sub> bond in 3 is shorter than that in 1, despite the fact that Si1 bears two fluorine atoms in both cases: the reason resides in the difference in the number of fluorine atoms on the Si2 atom. The exocyclic apical bond, Si2-F4<sub>ap</sub> = 1.672 Å, in 3 is much longer than the corresponding bond in 1 and 2: the Si2-F4<sub>ap</sub> bond in 3 appears to be elongated through interaction with the K<sup>+</sup> ion.

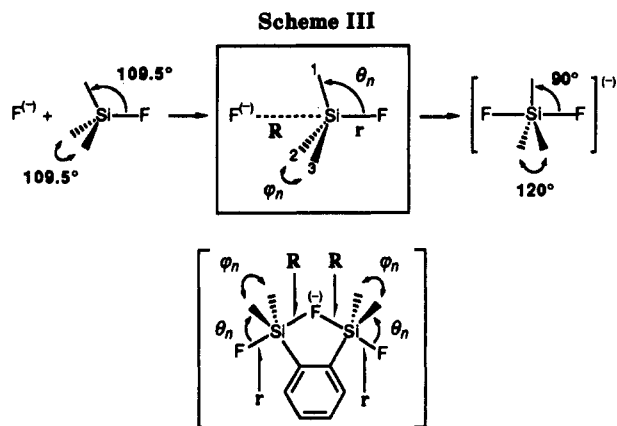
Silicon-equatorial atom bond lengths, Si-F<sub>eq</sub> and Si-C<sub>eq</sub>, in 1-3 are slightly shorter than those in a series of [Ar<sub>n</sub>SiF<sub>5-n</sub>]<sup>-</sup> compounds, including the typical example [Ph<sub>2</sub>SiF<sub>3</sub>]<sup>-</sup>: Si-F<sub>eq</sub> = 1.648 (2) Å and Si-C<sub>eq</sub> = 1.893 (2) Å.<sup>17</sup> Noteworthy is the presence of one of the shortest equatorial bonds for the series of organofluorosiliconates [R<sub>n</sub>SiF<sub>5-n</sub>]<sup>-</sup>: Si2-F4<sub>eq</sub> = 1.601 (4) Å in 1 and Si1-F2<sub>eq</sub> = 1.598 (4) Å in 2. The shortest Si-F<sub>eq</sub> distances reported so far are 1.597 (3) and 1.606 (2) Å in [PhSiF<sub>4</sub>]<sup>-</sup>,<sup>3</sup> while the perfluorosiliconate [SiF<sub>5</sub>]<sup>-</sup> has a much shorter Si-F<sub>eq</sub> bond, 1.579 Å.<sup>17</sup> These characteristic features concerning bond lengths imply that the geometry around the silicon atoms remains in the intermediate stages from TH to TBP. This point is discussed below.

**Bond Angles around the Silicon Atom and Pentacoordination Character.** It seems convenient to discuss the bond angles around the silicon atom in terms of pen-

(15) Tamao, K.; Hayashi, T.; Ito, Y.; Shiro, M. *Organometallics*, 1992, 11, 182.

(16) Cotton, F. A.; Wilkinson, G. In *Advanced Inorganic Chemistry*, 4th ed.; Wiley-Interscience: New York, 1980.

(17) Schormburg, D.; Krebs, R. *Inorg. Chem.* 1984, 23, 1378.



$$\text{Pentacoordination character (\% TBP}_a) = \frac{109.5^\circ - \frac{1}{3} \left( \sum_{n=1}^3 \theta_n \right)}{109.5^\circ - 90^\circ} \times 100 \quad (1)$$

$$\text{Pentacoordination character (\% TBP}_e) = \frac{120^\circ - \frac{1}{3} \left( \sum_{n=1}^3 \varphi_n \right)}{120^\circ - 109.5^\circ} \times 100 \quad (2)$$

tacoordination character, i.e., percent trigonal bipyramidal (% TBP),<sup>18</sup> since the geometry of the silyl groups in 1–3 is not a complete TBP but retains TH character to some extent, representing intermediate structures from TH to TBP. Our analysis is based on the concept developed by Dunitz.<sup>19</sup>

The pentacoordination character % TBP<sub>a</sub><sup>18</sup> may be defined by three apical-to-equatorial bond angles ( $\theta_n$ ,  $n = 1-3$ ) in an intermediate structure in which a nucleophile approaches along a vertical axis with retention of local  $C_3$  symmetry, as shown in Scheme III and eq 1; the bond angle ( $\theta_n$ ) varies from 109.5° in TH to 90° in TBP. Alternatively, % TBP<sub>e</sub> may also be defined by three equatorial-to-equatorial bond angles ( $\varphi_n$ ,  $n = 1-3$ ) which vary from 109.5° in TH to 120° in TBP, as shown in Scheme III and eq 2. In this model system,  $R$  and  $r$  denote respectively the Si–nucleophile distance and the opposite Si–leaving group distance. In the bis(siliconates), the angles  $\theta_n$  and  $\varphi_n$  correspond, respectively, to three exocyclic  $F_{ap}$ –Si–equatorial ligand angles and to three equatorial angles on each silicon atom, and the two distances  $R$  and  $r$  correspond to the Si– $F_{br}$  and the exocyclic Si– $F_{ap}$  bond lengths, respectively. Correlations between % TBP's and bond lengths will be discussed later. The displacement of the silicon atom ( $\Delta_{Si}$ ) from the equatorial plane is a criterion for deviation of the geometry from TBP to TH. The bond angles ( $\theta_n$  and  $\varphi_n$ ), pentacoordination characters (% TBP<sub>a</sub> and % TBP<sub>e</sub>), and  $\Delta_{Si}$  values are also listed in Table V.

**[F<sub>2</sub>{F}F<sub>2</sub>]<sup>−</sup> (1).** Si1 and Si2 atoms are displaced  $\Delta_{Si} = 0.131$  and  $0.205$  Å out of the  $F_{2eq}^1$ – $C_{1eq}$ – $C_{7eq}$  plane and the  $F_{4eq}^1$ – $C_{2eq}$ – $C_{13eq}$  plane to the direction of outside  $F_{3ap}^1$  and  $F_{5ap}^1$ , respectively, indicating residual tetrahedral character around the silicon atoms: in most of the known mono-(siliconates) of the  $[Ar_nSiF_{5-n}]^-$  type, the silicon is nearly in the equatorial plane,  $\Delta_{Si} = 0.02$ – $0.03$  Å.<sup>5,6,15</sup> On the Si1 side, the exocyclic apical–equatorial angles  $\theta_1$ – $\theta_3$ , i.e.,  $F_{3ap}^1$ –Si1– $F_{2eq}^1$ ,  $F_{3ap}^1$ –Si1– $C_{1eq}$ , and  $F_{3ap}^1$ –Si1– $C_{7eq}$ , are respectively 91.4, 95.3, and 96.1° (average 94.2°), while on

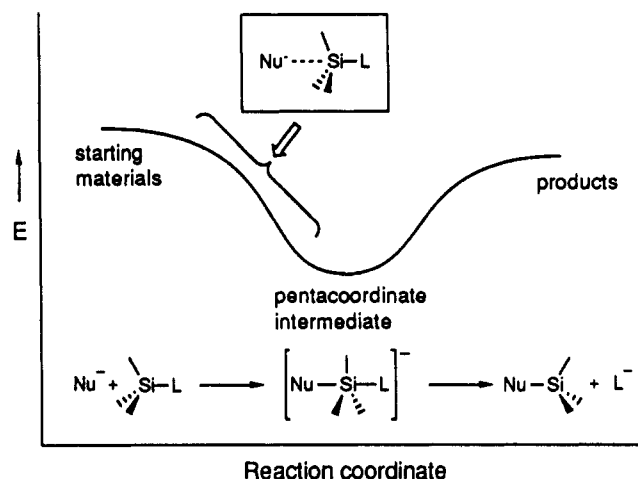


**Figure 4.** Schematic representation of the energy profile and intermediates in nucleophilic substitution at the tetracoordinate silicon center.

the Si2 side the corresponding angles are 94.6, 97.9, and 97.4° (average 96.6°). The % TBP<sub>a</sub> of Si1 and Si2 can thus be estimated by eq 1 to be 78% and 66%, respectively: the pentacoordination character is slightly greater in the former than in the latter. Alternatively, on the basis of the equatorial angles  $\varphi_1$ – $\varphi_3$  (average 119.5 and 118.7° for Si1 and Si2, respectively), the % TBP<sub>e</sub> may be estimated by eq 2 to be 95% and 88%, respectively: the % TBP<sub>e</sub> is much larger than the corresponding % TBP<sub>a</sub> obtained above.

**[F{F}F<sub>3</sub>]<sup>−</sup> (2).** The deviations  $\Delta_{Si}$  are 0.040 Å at Si1 and 0.314 Å at Si2. The averaged angles  $\theta_n$  on the Si1 and Si2 sides are 91.3 and 99.7°, respectively. Thus, the Si1 group has a nearly TBP geometry, 93% TBP<sub>a</sub>, while the Si2 group is only 50% TBP<sub>a</sub>. The difference in % TBP<sub>a</sub> between Si1 and Si2 is the largest of the three compounds. By the alternative description, Si1 and Si2 are 99 and 73% TBP<sub>e</sub>, respectively.

**[F{F}F<sub>2</sub>]<sup>−</sup> (3).** The deviation  $\Delta_{Si}$  is 0.078 Å for Si1 and 0.207 Å for Si2, respectively. The average of the apical–equatorial angles at the Si1 side is 92.4°, while these angles at the Si2 side average 96.3°, corresponding to 88% TBP<sub>a</sub> and 68% TBP<sub>a</sub> for Si1 and Si2, respectively. Alternatively, the % TBP<sub>e</sub> is 98% and 88% for Si1 and Si2, respectively.

It may be noted that the % TBP<sub>a</sub> of Si2 in 3 (68%) is larger than that of Si2 in 2 (50%), although the Si2 sides in 2 and 3 are regarded as the same  $[Ar_2SiF_2]^-$  moiety. Apparently, the silicon geometry is affected by the number of fluorine atoms on the other silicon atom in the bis-(siliconate) systems. Thus, the more fluorine atoms are present on silicon, the stronger the Lewis acidity of the silicon center results to attract a fluoride ion more tightly.

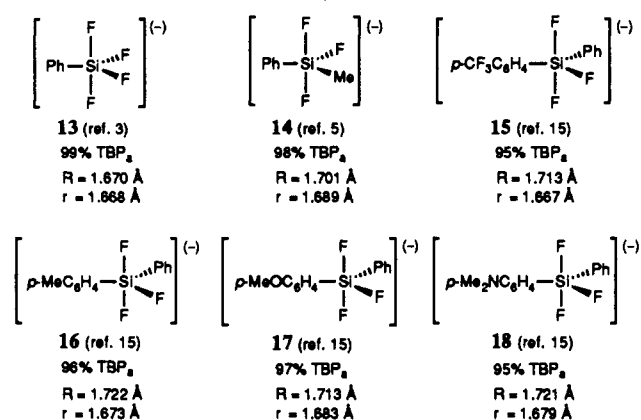
**Visual, Sequential Models for Structural Change from Tetrahedral to Trigonal Bipyramidal in Nucleophilic Attack on the Silicon Atom.** Pentacoordinate anionic siliconates have been designated as models for the intermediates in nucleophilic substitution at silicon,<sup>2</sup> the energy profile being illustrated in Figure 4.<sup>20</sup> Most of the previous experimental and theoretical studies have been devoted to the “regular” pentacoordinate siliconates corresponding to the bottom of the energy profile. Little information has been obtained on the structures in the intermediate stages from tetrahedral

(18) Although the pentacoordination character may be represented by % (TH→TBP), we prefer to use % TBP for brevity.

(19) Such an approach has been developed by Dunitz for coordination compounds of tin and sulfur derivatives: Bürgi, H.-B.; Dunitz, J. *Acc. Chem. Res.* 1983, 16, 153.

(20) (a) Sini, G.; Ohanessian, G.; Hiberty, P. C.; Shaik, S. S. *J. Am. Chem. Soc.* 1990, 112, 1407 and references cited therein. (b) Dewar, M. J.; Healy, E. *Organometallics* 1982, 1, 1706. (c) Wilhite, D. L.; Spialter, L. *J. Am. Chem. Soc.* 1973, 95, 2150.

Chart II



silane to trigonal-bipyramidal siliconate, corresponding to the slope region of the energy profile. Only a few reports have discussed such structural changes in "neutral" pentacoordinate species such as silatranes,<sup>21a-c</sup> 1-silyl-1,10-phenanthroline,<sup>21d</sup> and 8-amino-1-naphthylsilane<sup>21e</sup> derivatives which involve an intramolecular N→Si interaction. Quite recently, Bassindale and his co-workers have presented *N*-(silylmethyl)pyridones as sequential models for nucleophilic substitution at silicon involving an intramolecular O→Si interaction, as inferred by <sup>29</sup>Si NMR chemical shifts.<sup>22</sup>

The present bis(siliconates) 1–3 provide the first sequential models for structural change from TH to TBP in nucleophilic attack on silicon by an anionic nucleophile, F<sup>-</sup>, since F<sub>br</sub> and F<sub>ap</sub> are regarded as a nucleophile and a leaving group, respectively (cf. Scheme III). Now we find that there are linear relationships between % TBP<sub>a</sub> and bond lengths Si–F<sub>br</sub>(*R*) and Si–F<sub>ap</sub>(*r*), as shown in Figure 5: similar plots for Si–F<sub>eq</sub> and Si–C<sub>eq</sub> give a nearly flat lines (not shown). In order to examine the validity of the present analysis, we have applied a similar analysis to the typical anionic mono(siliconates) [R<sub>n</sub>SiF<sub>5-n</sub>]<sup>-</sup> (13–18 with little deformation by steric congestion; the structure, % TBP<sub>a</sub>, and Si–F<sub>ap</sub>(*R*) and Si–F<sub>eq</sub>(*r*) bond lengths are listed in Chart II. A plot of these data (open circles and open triangles) shows a good fit with the two lines derived above, as shown in Figure 5 (correlation factor *r* = 0.99 and 0.83, respectively).

A plot of Si–F<sub>br</sub>(*R*) vs the alternative pentacoordination character % TBP<sub>e</sub> results in a nonlinear correlation, as shown in Figure 5. This must be attributable to much larger values of % TBP<sub>e</sub> in comparison with the corresponding % TBP<sub>a</sub>. Thus, the % TBP<sub>e</sub> seems to be much more sensitive, especially in the final stages, to the bond angle changes, because the overall bond angle change from TH to TBP (10.5° from 109.5 to 120°) is only about half of that for % TBP<sub>a</sub> (19.5° from 109.5 to 90°).

In the sequential models, the structure changes in the order (A) Si2 in 2 (50% TBP<sub>a</sub> or 73% TBP<sub>e</sub>), (B) Si2 in 1 (66% TBP<sub>a</sub> or 88% TBP<sub>e</sub>), (C) Si2 in 3 (68% TBP<sub>a</sub> or

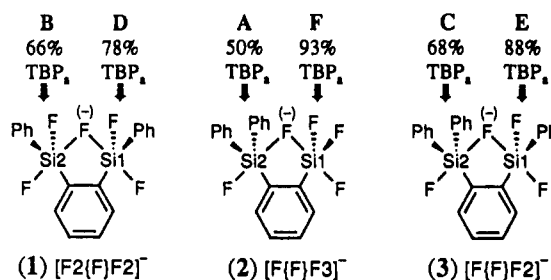
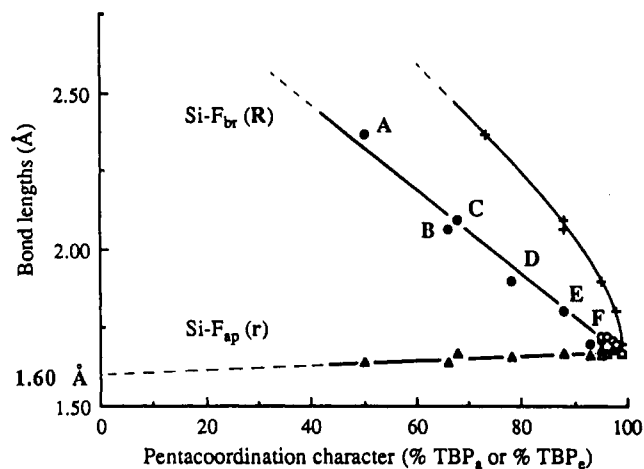


**Figure 5.** Plots of bond lengths vs pentacoordination characters in bis(siliconates) 1–3. The filled circles and triangles refer to Si–F<sub>br</sub>(*R*) and Si–F<sub>ap</sub>(*r*) vs % TBP<sub>a</sub>. The open circles and triangles refer to the long and the short Si–F<sub>ap</sub> bonds, respectively, in mono(siliconates) 13–18. The dotted line represents extrapolation to 0% TBP<sub>a</sub>. The cross marks refer to the plot of Si–F<sub>br</sub>(*R*) vs % TBP<sub>e</sub>.

88% TBP<sub>e</sub>), (D) Si1 in 1 (78% TBP<sub>a</sub> or 95% TBP<sub>e</sub>), (E) Si1 in 3 (88% TBP<sub>a</sub> or 98% TBP<sub>e</sub>), and (F) Si1 in 2 (93% TBP<sub>a</sub> or 99% TBP<sub>e</sub>), as illustrated in Figure 5. The final model species may have the TBP structure corresponding to the bottom of the valley of the reaction profile in Figure 4. Thus, during the process from 50% TBP<sub>a</sub> to 93% TBP<sub>a</sub> or from 73% TBP<sub>e</sub> to 99% TBP<sub>e</sub>, the Si–F<sub>br</sub> bond (=Si–nucleophile distance) shortens by 0.67 Å from 2.369 to 1.700 Å, while the Si–F<sub>ap</sub> bond (=Si–leaving group distance) is elongated by only 0.03 Å from 1.639 to 1.667 Å: the rather small change in the Si–F<sub>ap</sub> bond length may suggest a better fit with % TBP<sub>e</sub>. The equatorial bond lengths Si–F<sub>eq</sub> and exocyclic Si–C<sub>eq</sub> show only 0.01–0.02 Å elongation with variation of pentacoordination character.

Extrapolation of the line for Si–F<sub>ap</sub>(*r*) in Figure 5 to 0% TBP should converge on the Si–F bond length for tetrahedral organofluorosilanes. The extrapolated value (1.60 Å) is certainly almost same as the experimental data (1.59 Å or less).<sup>21e</sup> Although extrapolation of the lines for Si–F<sub>br</sub>(*R*) to 0% TBP may afford information on "incipient stages of chemical reaction",<sup>19</sup> whether linear or nonlinear extrapolation provides more accurate information must wait for further study on bis(siliconates) to fill blanks below 50% TBP<sub>a</sub> or 73% TBP<sub>e</sub>.

Finally, it should be mentioned that our compounds would not necessarily be the ideal model systems for such analysis, in view of the following (at least) two reasons. (1) Although the compounds involve three types of fluoro-siliconate moieties with variation of the number of fluorine atoms, the estimated % TBP's are plotted all together in one line. (2) The model nucleophile is not a free fluoride ion but a complexed ion; the nucleophilicity of the attacking fluoride ion is thus influenced by the nature of the neighboring silicon atom. We are now designing new types

(21) (a) Barrow, M. J.; Ebsworth, E. A. V.; Harding, M. M. *J. Chem. Soc., Dalton Trans.* 1980, 1838. (b) Pestunovich, V. A.; Sidorkin, V. F.; Dogaev, O. B.; Voronkov, M. G. *Dokl. Akad. Nauk SSSR* 1980, 251, 1440. (c) Voronkov, M. G.; Dyakov, V. M.; Kirpichenko, S. V. *J. Organomet. Chem.* 1982, 233, 1. (d) Klebe, G. *J. Organomet. Chem.* 1985, 293, 147. (e) Brelriere, C.; Carre, F.; Corriu, R. J. P.; Poirier, M.; Royo, G.; Zwecker, J. *Organometallics* 1989, 8, 1831. (f) Sheldrick, W. S. In *The Chemistry of Organic Silicon Compounds*; Patai, S., Rappoport, Z., Eds.; Wiley: Chichester, U.K., 1989; Part 1, Chapter 3.

(22) Bassindale, A.; Borbaruah, M. 9th International Symposium on Organosilicon Chemistry, Edinburgh, UK, July 16–20, 1990; Abstract B.13.

of bis(siliconates) containing a constant number of fluorines for further analysis.

**III. Solution Structures by NMR Studies.** NMR spectroscopy is a powerful method for the characterization of pentacoordinate siliconates in solution.<sup>1</sup> <sup>19</sup>F NMR studies on fluorosiliconates reported by Klanberg and Muetterties,<sup>23</sup> Damrauer and his co-workers,<sup>4</sup> and Holmes and his co-workers<sup>5,6</sup> have accumulated the following significant results. Organotetrafluorosiliconates<sup>6,24</sup> [RSiF<sub>4</sub>]<sup>-</sup> and diorganotrifluorosiliconates<sup>4,6</sup> [R<sub>2</sub>SiF<sub>3</sub>]<sup>-</sup> undergo fast ligand exchange by Berry pseudorotation<sup>24</sup> at room temperature or above to show a singlet due to all fluorine atoms. The <sup>19</sup>F chemical shifts for [RSiF<sub>4</sub>]<sup>-</sup> and [R<sub>2</sub>SiF<sub>3</sub>]<sup>-</sup> are on average around -116 and -103 ppm, being 24 and 36 ppm downfield from those of the tetracoordinate precursors RSiF<sub>3</sub> and R<sub>2</sub>SiF<sub>2</sub>, respectively.<sup>6</sup> The dynamic behavior greatly depends on the number of fluorine atoms on silicon. Thus, in the case of trifluorosiliconates [R<sub>2</sub>SiF<sub>3</sub>]<sup>-</sup>, when the temperature was lowered, the averaged fluorine signal broadened and separated into two peaks assignable to two apical (average -89 ppm) and one equatorial (average -133 ppm) fluoride ligand in a TBP structure.<sup>6b</sup> The energy barriers to the ligand exchange processes are range from 9 to 14 kcal/mol, depending on the steric and/or electronic effects of organic groups. In the case of tetrafluorosiliconates [RSiF<sub>4</sub>]<sup>-</sup> the ligand-exchange process is usually too fast to observe the static spectra at low temperatures,<sup>4a,6b</sup> except for one example, [(TTBP)SiF<sub>4</sub>]<sup>-</sup>, which has the energy barrier for F exchange of 12.8 kcal/mol.<sup>6b</sup> In contrast to the above two types of anionic siliconates, difluorosiliconate [Ph<sub>3</sub>SiF<sub>2</sub>]<sup>-</sup> shows no dynamic behavior even at ambient temperature or above,<sup>4a</sup> indicating the high stability of the TBP structure with three organic groups at equatorial positions and two fluorines at apical positions.

<sup>29</sup>Si and <sup>13</sup>C NMR studies on pentacoordinate anionic siliconates have been limited so far. Holmes and his co-workers recently presented an empirical rule that the <sup>29</sup>Si chemical shifts of anionic siliconates [RSiF<sub>4</sub>]<sup>-</sup> (average -126 ppm) and [R<sub>2</sub>SiF<sub>3</sub>]<sup>-</sup> (average -90 ppm) are upfield by about 51 and 71 ppm on average in comparison with those of the fluorosilane precursors RSiF<sub>3</sub> and R<sub>2</sub>SiF<sub>2</sub>, respectively.<sup>6</sup> They also observed, for the first time, retention of <sup>29</sup>Si-<sup>19</sup>F spin-spin coupling by variable-temperature <sup>29</sup>Si NMR spectroscopy of [R<sub>2</sub>SiF<sub>3</sub>]<sup>-</sup> and [(TTBP)SiF<sub>4</sub>]<sup>-</sup> to confirm the intramolecularity of the exchange process.<sup>6</sup> We have carried out <sup>13</sup>C NMR studies on a series of [Ar<sub>2</sub>SiF<sub>3</sub>]<sup>-</sup> compounds in detail to show, for the first time, that the <sup>13</sup>C chemical shifts of Si-*ipso* carbons of aryl groups are about 20 ppm downfield from those of the fluorosilane precursors Ar<sub>2</sub>SiF<sub>2</sub> and are influenced by the electronic effects of the para substituent.<sup>15</sup> For example, the <sup>13</sup>C NMR spectrum of [Ph<sub>2</sub>SiF<sub>3</sub>]<sup>-</sup> exhibits a quartet due to the *ipso* carbon at 148.40 ppm (<sup>2</sup>J<sub>CF</sub> = 34.88 Hz) and a narrower quartet due to ortho carbons at 138.41 ppm (<sup>3</sup>J<sub>CF</sub> = 4.75 Hz). The above significant information obtained

**Table VI.** <sup>19</sup>F NMR Spectroscopic Data for Siliconates and Fluorosilanes in Acetone-*d*<sub>6</sub> at 20 °C

siliconate <sup>a</sup>	chem shift, ppm <sup>b</sup>
[F <sub>2</sub> {F}F <sub>2</sub> ] <sup>-</sup> (anion of 1)	-117.3 (broad singlet, 5 F)
[F{F}F <sub>3</sub> ] <sup>-</sup> (anion of 2)	-116.9 (sharp singlet, 4 F) <sup>c</sup> -133.9 (sharp singlet, 1 F)
[F{F}F <sub>2</sub> ] <sup>-</sup> (anion of 3)	-111.4 (broad singlet, 4 F) <sup>d</sup>
[Ph <sub>2</sub> SiF <sub>3</sub> ] <sup>-</sup>	-111.2 (broad singlet, 3 F) <sup>e</sup>
[PhSiF <sub>4</sub> ] <sup>-</sup>	-118.1 (sharp singlet, 4 F) <sup>f</sup>
PhSiF <sub>3</sub>	-140.90 <sup>g</sup>
Ph <sub>2</sub> SiF <sub>2</sub>	-141.69 <sup>g</sup>
Ph <sub>3</sub> SiF	-169.14 <sup>g</sup>

<sup>a</sup>The counteranion for siliconate is K<sup>+</sup>-18-crown-6. <sup>b</sup>Chemical shifts are referenced to CFC<sub>3</sub>. <sup>c</sup>J<sub>SIF</sub> = 207.0 Hz. <sup>d</sup>At +50 °C. <sup>e</sup>Lit.<sup>4a</sup> -110.7 ppm in acetone-*d*<sub>6</sub> at +38 °C. <sup>f</sup>Lit.<sup>6b</sup> -114.3 ppm in CDCl<sub>3</sub> at -18.2 °C. <sup>g</sup>Sharp singlet.

**Table VII.** <sup>13</sup>C NMR Spectroscopic Data for Bis(siliconates) 1-3 in Acetone-*d*<sub>6</sub> at 24 °C<sup>a</sup>

	i: 149.03 (sextet, <sup>2</sup> J <sub>CF</sub> = 16.86) o: 136.75 (sextet, <sup>3</sup> J <sub>CF</sub> = 2.64) m: 127.29 (singlet) p: 128.90 (singlet) i': 142.02 (sextet, <sup>2</sup> J <sub>CF</sub> = 19.06) o': 138.49 (sextet, <sup>3</sup> J <sub>CF</sub> = 3.85) m: 129.62 (broad singlet)
	i: 141.85 (multiplet) o: 136.36 (sextet, <sup>3</sup> J <sub>CF</sub> = 2.26) m: 127.37 (singlet) p: 128.63 (singlet) i', i'': 148.5 (multiplet) o', o'': 137.45 (multiplet), 139.78 (sextet, <sup>3</sup> J <sub>CF</sub> = 4.04) m', m'': 129.12 (broad singlet), 129.66 (broad singlet)
	ii: 149.33 (quintet, <sup>2</sup> J <sub>CF</sub> = 12.40) oi: 137.20 (multiplet) m1: 126.80 (singlet) p1: 127.96 (singlet) i2: 143.45 (quintet, <sup>2</sup> F <sub>CF</sub> = 14.33) o2: 136.67 (multiplet) m2: 127.16 (singlet) p2: 128.12 (singlet) i': 144.34 (quintet, <sup>3</sup> J <sub>CF</sub> = 25.48) i'': 151.66 (quintet, <sup>3</sup> J <sub>CF</sub> = 23.69) o', o'': 138.00 (multiplet), 139.52 (multiplet) m', m'': 128.86 (broad singlet), 129.05 (broad singlet)

<sup>a</sup>At 100.59 MHz. Chemical shifts are referenced to Me<sub>4</sub>Si. Chemical shifts are given in ppm and J values in Hz. <sup>13</sup>C chemical shifts of the counteranion, K<sup>+</sup>-18-crown-6, for 1-3 are 70.70, 70.79, and 70.82 ppm, respectively.

from the NMR study of mono(siliconates) was extremely useful for the analysis of the structure and dynamic behavior of bis(siliconates).

**(A) NMR Studies at Ambient Temperatures.** <sup>19</sup>F NMR Spectroscopy. <sup>19</sup>F NMR data at room temperature for 1-3 are summarized in Table VI (the spectra are reproduced in Figures 8, 10, and 11, which will be discussed later in the variable-temperature <sup>19</sup>F NMR section). A single broad signal for [F<sub>2</sub>{F}F<sub>2</sub>]<sup>-</sup> (1) observed at -117.3 ppm indicates a fast intramolecular exchange process of all five fluorine nuclei. [F{F}F<sub>2</sub>]<sup>-</sup> (3) also showed a broad single peak at -111.4 ppm at room temperature due to four fluorines on two silicon atoms. In contrast, [F{F}F<sub>3</sub>]<sup>-</sup> (2) gives two sharp peaks in the ratio of 4:1 at -116.9 and -133.9 ppm. This indicates that the four fluorine atoms at the -SiF<sub>4</sub><sup>-</sup> part undergo a fast intramolecular exchange at ambient temperature, while the remaining fluorine on

(23) Klanberg, F.; Muetterties, E. L. *Inorg. Chem.* 1968, 7, 155.

(24) The first experimental evidence for pseudorotation of neutral pentacoordinate fluorosilanes has been presented by Corriu and his co-workers: (a) Corriu, R. J. P.; Kpton, A.; Poirier, M.; Royo, G.; Corey, J. Y. *J. Organomet. Chem.* 1984, 277, C25. (b) Corriu, R. J. P.; Mazhar, M.; Poirier, M.; Royo, G. *J. Organomet. Chem.* 1986, 306, C5. Martin and his co-workers reported the energetics of and electronic effects on pseudorotation of anionic cyclic alkoxy-siliconates: (c) Stevenson, W. H., III; Wilson, S.; Martin, J. C.; Farnham, W. B. *J. Am. Chem. Soc.* 1985, 107, 1985. (d) Stevenson, W. H., III; Martin, J. C. *J. Am. Chem. Soc.* 1985, 107, 6352. Pseudorotation has recently been reconsidered theoretically: (e) Gordon, M. S.; Windus, T. L.; Burggraf, L. W.; Davis, L. P. *J. Am. Chem. Soc.* 1990, 112, 7167. (f) Windus, T. L.; Gordon, M. S.; Burggraf, L. W.; Davis, L. P. *J. Am. Chem. Soc.* 1991, 113, 4357.



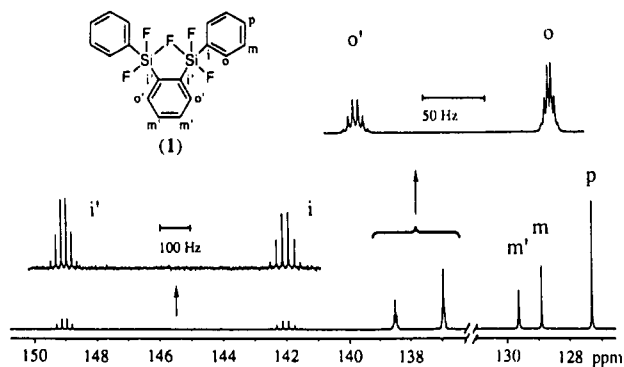


**Figure 6.**  $^{13}\text{C}$  NMR signals for aromatic carbons in **1** at 24 °C (100.59 MHz, acetone- $d_6$ , standard TMS).

$-\text{SiPh}_2\text{F}$  does not exchange with the other four fluorine atoms. The fluorine chemical shift of the  $-\text{SiPh}_2\text{F}$  group is, however, downfield by 35.2 ppm from that of  $\text{Ph}_3\text{SiF}$ , suggesting interaction between the  $-\text{SiPh}_2\text{F}$  and  $-\text{SiF}_4^-$  moieties in **2**.

**$^{13}\text{C}$  NMR Spectroscopy.** All carbons in **1–3** were assigned by the coupling patterns with fluorine atoms on each silicon, peak intensities, and two-dimensional H-C COSY spectra.  $^{13}\text{C}$  data for bis(silicates) **1–3** and the spectrum of **1** are shown in Table VII and in Figure 6, respectively.

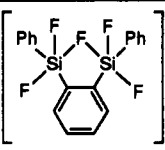
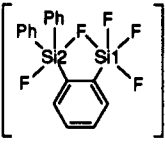
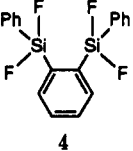
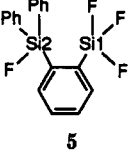
The  $^{13}\text{C}$  NMR spectrum of "symmetrical"  $[\text{F}_2\{\text{F}\}\text{F}_2]^-$  (**1**) shows two sextets due to two kinds of ipso carbons  $\text{C}_i$  in the core benzene ring at 142.04 ppm and  $\text{C}_i$  in the two phenyl groups at 149.03 ppm and two narrower sextets due to two kinds of ortho carbons  $\text{C}_o$  at 138.49 ppm and  $\text{C}_o$  at 136.75 ppm. These  $^{13}\text{C}$  NMR data also demonstrate that all five fluorine atoms are equivalent on the  $^{13}\text{C}$  NMR time scale, in accordance with the  $^{19}\text{F}$  NMR behavior.

Similarly, in the unsymmetrical  $[\text{F}\{\text{F}\}\text{F}_2]^-$  (**3**), the carbon signals for the ipso positions appear as four quintets, indicating a fast exchange of all four fluorine nuclei.

The  $^{13}\text{C}$  NMR spectrum of unsymmetrical  $[\text{F}\{\text{F}\}\text{F}_3]^-$  (**2**) also indicates the presence of fluorine ligand exchange, but somewhat different behavior. Two of the three kinds of ortho carbons split into sextets due to coupling with five fluorine atoms, but the remaining ortho carbon and all of the ipso carbon signals are observed as multiplets or broad signals. Thus, the exchange rate at ambient temperature is comparable with or somewhat larger than the  $^{13}\text{C}$  NMR time scale. This observation may be consistent with the result of the  $^{19}\text{F}$  NMR study discussed above, in view of the relative dynamic resolution abilities in the ratio of  $^1\text{H}:\text{C}:\text{F} = 1:8:28$ .<sup>25</sup>

**$^{29}\text{Si}$  NMR Spectroscopy in Solution.** The  $^{29}\text{Si}$  chemical shift and coupling constant,  $J_{\text{SiF}}$ , for  $[\text{F}_2\{\text{F}\}\text{F}_2]^-$  (**1**) are compared with data for other pertinent compounds in Table VIII. Three significant features should be mentioned. (1) At 20 °C, the  $^{29}\text{Si}$  NMR peak appears as a sextet for two silicon atoms, consistent with the fast exchange of all five fluorine nuclei. (2) The  $^{29}\text{Si}$  chemical shift ( $\delta$  -90.03 ppm) of **1** is intermediate between those of the tetracoordinate precursors *o*-bis(difluorophenylsilyl)benzene (**4**;  $\delta$  -30.21 ppm) and  $\text{Ph}_2\text{SiF}_2$  ( $\delta$  -29.00 ppm) and that of the pentacoordinate mono(silicate)  $[\text{Ph}_2\text{SiF}_3]^-$  ( $\delta$  -109.55 ppm). (3) The Si-F coupling constant ( $J_{\text{SiF}} = 134.74$  Hz) is smaller than those of  $\text{Ph}_2\text{SiF}_2$  ( $J_{\text{SiF}} = 291.2$  Hz) and  $[\text{Ph}_2\text{SiF}_3]^-$  ( $J_{\text{SiF}} = 238.06$  Hz) and is comparable with the calculated average value (130 Hz) on the assumption of  $^1J_{\text{SiF}} = 291$  Hz ( $\times 2$  F),  $^1J_{\text{SiF}} = 238$  Hz ( $\times 3$  F),

**Table VIII.**  $^{29}\text{Si}$  NMR Spectroscopic Data for Bis(silicates) and Mono(silicates) and Their Precursors, Fluorosilanes, in Solution and/or in the Solid State<sup>a</sup>

silicate and precursor <sup>b</sup>	chem shift, ppm (multiplicity, coupling const, Hz) <sup>c</sup>
 anion of <b>1</b>	-90.03 (sextet, $J_{\text{SiF}} = 134.74$ ) [-75 to -105 (multiplet)] <sup>d</sup>
 anion of <b>2</b> <sup>e</sup>	[-129.3 (Si1, triplet, $J_{\text{SiF}} = 207.9$ ), -31.3 (Si2, doublet, $J_{\text{SiF}} = 256.5$ )] <sup>d</sup>
 <b>4</b>	-30.21 (triplet, $J_{\text{SiF}} = 293.9$ Hz)
 <b>5</b>	-73.46 (Si1, quintet, $J_{\text{SiF}} = 265.4$ ), -3.63 (Si2, doublet, $J_{\text{SiF}} = 282.1$ )
$[\text{Ph}_2\text{SiF}_3]^-$	-109.55 (quartet, $J_{\text{SiF}} = 238.06$ ) <sup>f</sup>
$[\text{PhSiF}_4]^-$	-125.90 (quintet, $J_{\text{SiF}} = 210$ ) <sup>g</sup> [-129.28 (triplet, $J_{\text{SiF}} = 200.2$ )] <sup>d</sup>
$\text{Ph}_2\text{SiF}_2$	-29.00 (triplet, $J_{\text{SiF}} = 291.20$ )
$\text{PhSiF}_3$	-72.42 (quintet, $J_{\text{SiF}} = 266.8$ )

<sup>a</sup>Spectra were recorded at 20 °C in acetone- $d_6$ , unless otherwise stated. Solid-state spectral data are given in brackets. <sup>b</sup>The counteranion of silicate is  $\text{K}^+$ -18-crown-6. <sup>c</sup>Chemical shifts are referenced to TMS in solution and to DSS in the solid state. <sup>d</sup>Solid-state data. <sup>e</sup>No signal in solution. <sup>f</sup>Lit.<sup>6c</sup> -106.4 ppm ( $J = 238$  Hz) in  $\text{CD}_2\text{Cl}_2$ . <sup>g</sup>Literature data measured in  $\text{CD}_2\text{Cl}_2$ .<sup>6b</sup>

and  $^4J_{\text{SiF}} = 0$  ( $\times 5$  F). Thus, these data strongly support fast fluoride transfer between tetracoordinate and pentacoordinate silicon atoms: the mechanisms of the fluorine exchange will be discussed later. The unsymmetrical bis(silicates) **2** and **3** showed no detectable peaks of the silicon nuclei in solution.

**Solid-State  $^{29}\text{Si}$  NMR Spectroscopy.** Solid-state MAS  $^{29}\text{Si}$  NMR data for the pentacoordinate bis(silicates) **1** and **2** and mono(silicate)  $[\text{PhSiF}_4]^-$ ,  $\text{K}^+$ -18-crown-6 are also summarized in Table VIII for comparison. The solid-state spectrum of **1** shows an uncharacterizable multiplet, possibly due to the slightly unsymmetrical structure. In contrast to no peak in solution, the solid-state spectrum of  $[\text{F}\{\text{F}\}\text{F}_3]^-$  (**2**) shows two distinct silicon peaks at -31.30 ppm as a doublet ( $^1J_{\text{SiF}} = 256.5$  Hz) for Si2 and at -129.32 ppm as a triplet ( $^1J_{\text{SiF}} = 207.9$  Hz) for Si1, as shown in Table VIII and in Figure 7. While Si2 couples with only one fluorine, the Si1 couples with only two of the four fluorines on Si1 to appear as a triplet. It may be noted here that the silicon atom in the mono(silicate)  $[\text{PhSiF}_4]^-$  also appears as a triplet in the solid state (Table VIII), although it cannot readily be deduced whether the triplet arises from coupling with two apical or two equatorial fluorines. The Si1 signal of **2** appears ca. 56 ppm upfield from that of the  $-\text{SiF}_3$  group in the precursor *o*-(fluorodiphenylsilyl)(trifluorosilyl)benzene (**5**). This dif-

(25) Martin, M. L.; Martin, G. J.; Delpuech, J.-J. *Practical NMR Spectroscopy*; Heyden & Son: London, 1980; p 311.

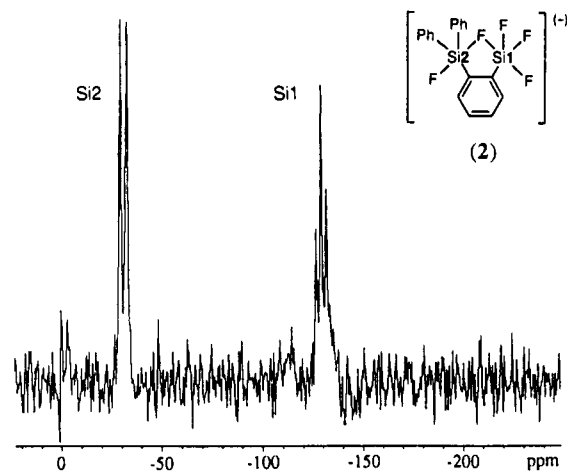


Figure 7. Solid-state  $^{29}\text{Si}$  NMR spectrum for **2** (79.46 MHz, external standard DSS at  $\delta$  0 ppm).

ference is nearly equal to that (56.8 ppm) between  $[\text{PhSiF}_4]^-$  in the solid state and  $\text{PhSiF}_3$  in acetone- $d_6$ , as shown in Table VIII. Similarly, the chemical shift of Si2 in **2** also shows a 27.7 ppm upfield shift from that of the  $-\text{SiPh}_2\text{F}$  group in **5**, but the chemical shift difference is less than half of that for Si1. Thus, it may be deduced that the Si1 side is almost completely pentacoordinated, as for the trigonal-bipyramidal mono(silicate)  $[\text{PhSiF}_4]^-$ , while the Si2 side is of low pentacoordination character, in accordance with the results obtained by X-ray structural analysis.

The  $^{29}\text{Si}$ - $^{19}\text{F}$  spin-spin coupling constant observed in the solid-state  $^{29}\text{Si}$  NMR spectrum also provides useful information on the degree of interaction of the bridging fluorine atom with silicon atoms, i.e., pentacoordination character.  $^1J_{\text{Si1F}}$  in the bis(silicate) **2** and  $^1J_{\text{Si1F}}$  in the precursor **5** are 207.9 and 265.4 Hz, respectively. Thus, the coupling constant in **2** is 57.5 Hz smaller than that in **5**. This suggests that Si1 in **2** is highly pentacoordinated, since the difference in  $^1J_{\text{SiF}}$  between  $[\text{PhSiF}_4]^-$  and  $\text{PhSiF}_3$  is 66.5 Hz.<sup>26</sup> In contrast, the coupling constant of  $^1J_{\text{Si2F}}$  in **2** is 256.5 Hz, which is 25.6 Hz smaller than  $^1J_{\text{Si2F}} = 282.1$  Hz in **5**, suggesting lower pentacoordination character of Si2 in **2**. On the basis of the X-ray structural analysis of **2**, pentacoordination characters of Si1 and Si2 have been estimated to be 93% and 50%, respectively. Thus, the geometries about silicon atoms estimated from the  $^{29}\text{Si}$  chemical shifts and  $^{29}\text{Si}$ - $^{19}\text{F}$  coupling constants by solid-state  $^{29}\text{Si}$  NMR spectroscopy are consistent with the geometries found by the X-ray structural analysis.

**(B) Variable-Temperature  $^{19}\text{F}$  NMR Spectroscopy and Mechanisms of Ligand Exchange.** The  $^{19}\text{F}$  NMR chemical shifts of bis(silicates) **1**-**3** at low-temperature limits are summarized in Table IX, which contains some other pertinent data for comparison. The variable-temperature  $^{19}\text{F}$  NMR spectra for **1**-**3** are shown in Figures 8-11. The spectral changes will be explained by the following four processes: (a) exchange of the bridging fluorine  $\text{F}_{\text{br}}$  between tetracoordinate and pentacoordinate silicon atoms (abbreviated as " $\text{F}_{\text{br}}$  exchange"), (b) flipping of the  $\text{F}_{\text{br}}$ -containing five-membered ring, caused by partial rotation about the two endocyclic Si-C bonds (abbreviated as "flipping"), (c) full rotation about the endocyclic Si-C bonds (abbreviated as "Si-C rotation"), and (d) pseudorotation at pentacoordinate silicon centers (abbreviated as "pseudorotation"). A detailed discussion will be pres-

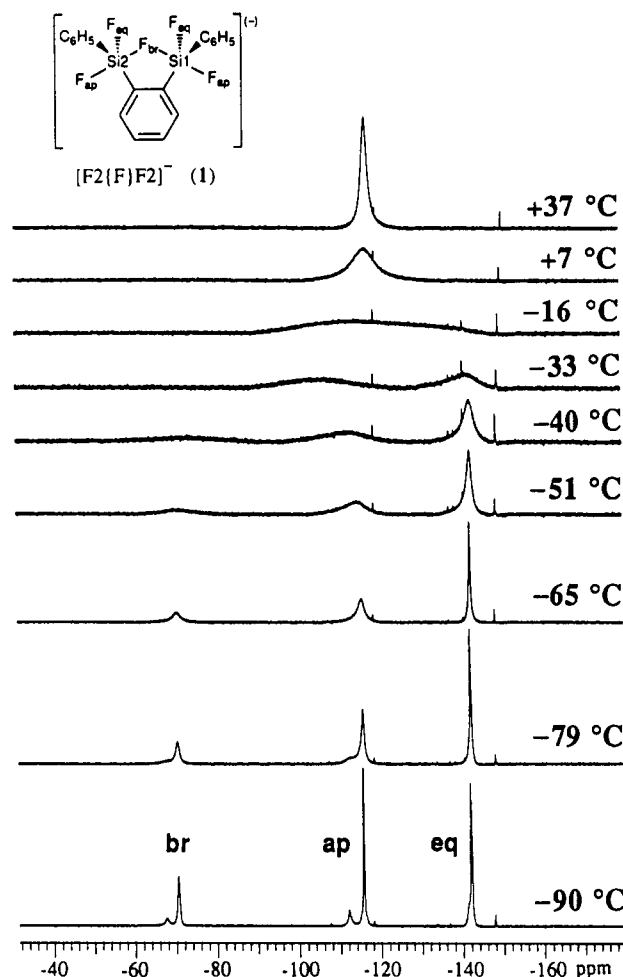


Figure 8. Stacked plot of the variable-temperature  $^{19}\text{F}$  NMR spectra for **1** (185.15 MHz, acetone- $d_6$ , internal standard  $\text{CFCl}_3$  at  $\delta$  0 ppm). Two small signals around -118 and -148 ppm are due to impurities.

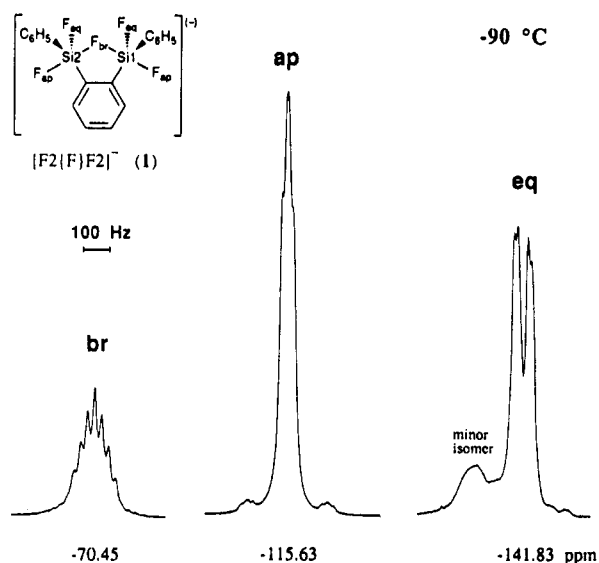


Figure 9. Expanded  $^{19}\text{F}$  NMR signals for the major isomer of **1** recorded at  $-90^\circ\text{C}$  in acetone- $d_6$  (internal standard  $\text{CFCl}_3$  at  $\delta$  0 ppm). The side bands of the  $\text{F}_{\text{ap}}$  signal are due to  $^{19}\text{F}$ - $^{29}\text{Si}$  coupling.

ented for **1**, which exhibits all of these processes; flipping has not been observed in **2** and **3**. The relative ease of processes a-d depends on the number of fluorine atoms. Since the behavior of compound **2** is rather different from

(26) Holmes reported  $J_{\text{SiF}}(\text{RSiF}_3\text{-RSiF}_4) = 58$  Hz.<sup>6b</sup>

Table IX.  $^{19}\text{F}$  Chemical Shifts in Siliconates at Low-Temperature Limits

siliconate <sup>a</sup>	temp, °C	chem shift, ppm (assign, coupling const, Hz) <sup>b</sup>
	-90	major isomer: -70.45 (F <sub>br</sub> , triple triplet, $J_{\text{F}_{\text{br}}\text{F}_{\text{eq}}} = 45$ , $J_{\text{F}_{\text{br}}\text{F}_{\text{ap}}} = 22$ ), -115.63 (F <sub>ap</sub> , tripletlike, $J_{\text{av}} = 17$ ), <sup>c,d</sup> -141.83 (F <sub>eq</sub> , double doublet, $J_{\text{F}_{\text{br}}\text{F}_{\text{eq}}} = 45$ , $J_{\text{F}_{\text{eq}}\text{F}_{\text{ap}}} = 12$ ) minor isomer: -67.64 (F <sub>br</sub> , broad), -111.91 (F <sub>ap</sub> , broad), -141.03 (F <sub>eq</sub> )
[F <sub>2</sub> F]F <sub>2</sub> <sup>-</sup> (anion of 1)	-110 <sup>e</sup>	-77.53 (F <sub>br</sub> , broad), -118.89 (F <sub>ap1</sub> , broad), -130.51 (F <sub>ap2</sub> ), -134.77 (F <sub>eq1</sub> , broad)
	-93	-70.40 (F <sub>br</sub> , broad), -108.49 (F <sub>ap1</sub> , broad), -126.62 (F <sub>ap2</sub> ), <sup>f</sup> -136.15 (F <sub>eq1</sub> ) <sup>g</sup>
[F]F]F <sub>2</sub> <sup>-</sup> (anion of 3)	-85	-99.55 (F <sub>ap</sub> ), -132.67 (F <sub>eq</sub> )
[Ph <sub>2</sub> SiF <sub>3</sub> ] <sup>-</sup>	-88	-77.98 (F <sub>ap</sub> ), -112.70 (F <sub>eq</sub> )
[(TTBP)SiF <sub>4</sub> ] <sup>-h</sup>		

<sup>a</sup> In acetone-*d*<sub>6</sub>, unless otherwise stated. The counteranion is K<sup>+</sup>-18-crown-6. <sup>b</sup> Chemical shifts are referenced to CFC<sub>3</sub>. <sup>c</sup> Tripletlike double doublet. Only the averaged coupling constant,  $J_{\text{av}} = (J_{\text{F}_{\text{br}}\text{F}_{\text{ap}}} + J_{\text{F}_{\text{ap}}\text{F}_{\text{eq}}})/2$ , was measurable. <sup>d</sup>  $J_{\text{FSi}} = 263.4$  Hz. <sup>e</sup> In THF-*d*<sub>8</sub>. <sup>f</sup>  $J_{\text{FSi}} = 259.1$  Hz. <sup>g</sup>  $J_{\text{FSi}} = 220.3$  Hz. <sup>h</sup> Literature data recorded in CD<sub>2</sub>Cl<sub>2</sub>; TTBP = 2,4,6-tri-*tert*-butylphenyl.<sup>6b</sup>

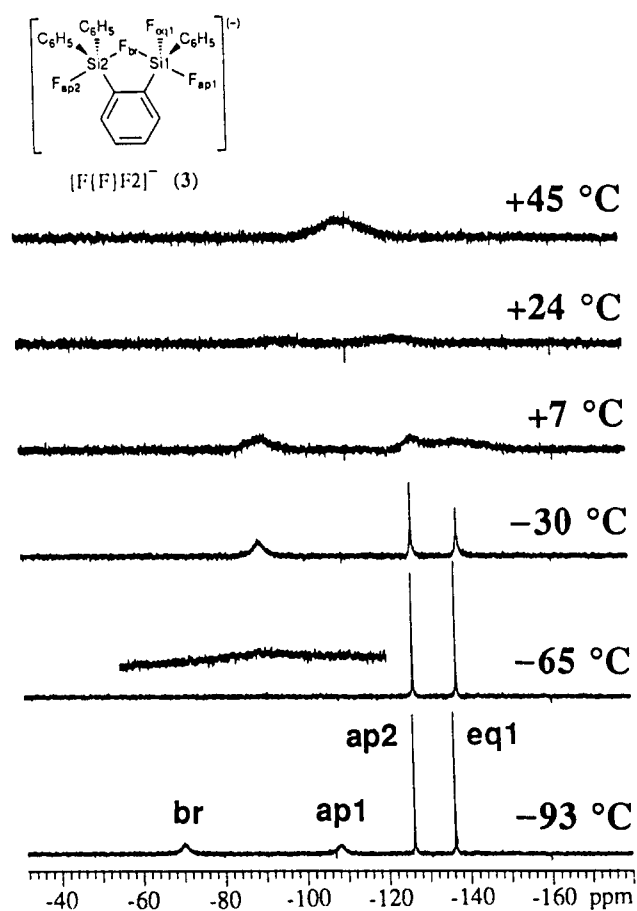


Figure 10. Stacked plot of the variable-temperature  $^{19}\text{F}$  NMR spectra for 3 (185.15 MHz, acetone-*d*<sub>6</sub>, internal standard CFC<sub>3</sub> at  $\delta$  0 ppm).

that of other two, the variable-temperature  $^{19}\text{F}$  NMR spectra will be discussed in the order of compounds 1, 3, and 2.

[F<sub>2</sub>F]F<sub>2</sub><sup>-</sup> (1). The  $^{19}\text{F}$  NMR spectra of 1 in acetone-*d*<sub>6</sub>, taken at temperature ranging from -90 to +37 °C, are

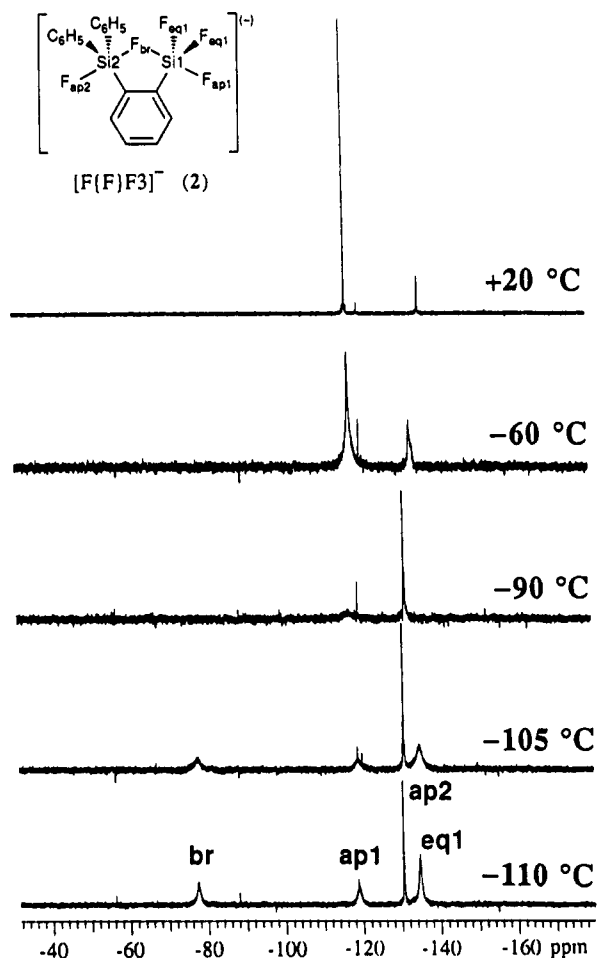
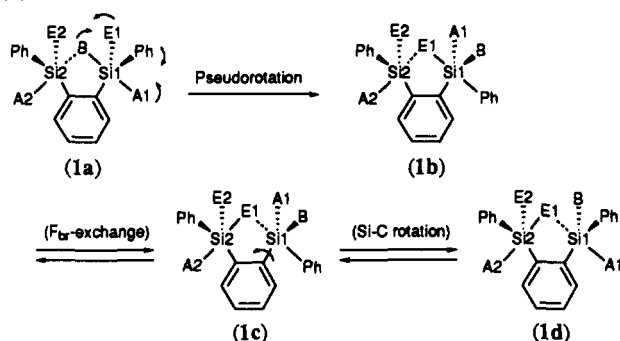


Figure 11. Stacked plot of the variable-temperature  $^{19}\text{F}$  NMR spectra for 2 (185.15 MHz, THF-*d*<sub>8</sub>, internal standard CFC<sub>3</sub> at  $\delta$  0 ppm). A small sharp signal around -119 ppm is due to an impurity.

shown in Figure 8. At -90 °C, three major signals due to F<sub>br</sub>, F<sub>ap</sub>, and F<sub>eq</sub> at around -70, -115, and -141 ppm, respectively, are accompanied by small signals each in the

Scheme IV<sup>a</sup>

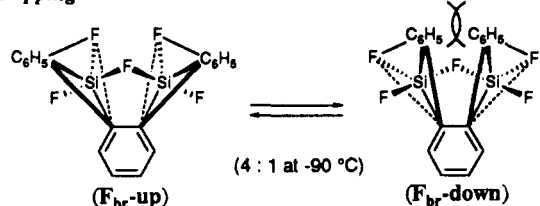
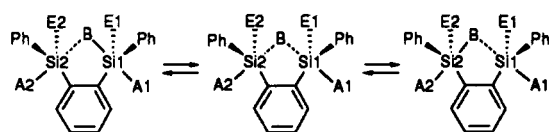
## (d) Pseudorotation



## (c) Si-C rotation



## (b) Flipping

(a) F<sub>br</sub>-exchange

<sup>a</sup> F<sub>br</sub>, F<sub>ap</sub>, and F<sub>eq</sub> are abbreviated B, A, and E, respectively, for clarity.

ratio of 4:1, indicating the presence of isomers; the full data are summarized in Table IX.<sup>27</sup> The assignment for F<sub>ap</sub> and F<sub>eq</sub> is based on the empirical rule for mono(silicates) that equatorial fluorines appear at higher fields, as mentioned above.<sup>5</sup> Upon an increase in the temperature, each pair coalesces into a single signal around -80 °C. The F<sub>br</sub> and F<sub>ap</sub> signals coalesce at -33 °C, leaving the F<sub>eq</sub> signal as a broad singlet, and finally coalescence of all signals is observed at -16 °C. These temperature-dependent spectra and the ground-state structure at the low-temperature limit (-90 °C) are explained by the four processes visualized in Scheme IV.

**F<sub>br</sub> Exchange (a).** The fluorine bridge seems to be "symmetrical" in solution at -90 °C, in contrast to the unsymmetrical structure in the solid state. This has been deduced from the analysis of the splitting patterns of three major signals in terms of an X<sub>2</sub>Y<sub>2</sub>Z five-spin system, where X, Y, and Z stand for F<sub>eq</sub>, F<sub>ap</sub>, and F<sub>br</sub>, respectively. Thus, the expanded spectra shown in Figure 9 indicate that the major signals for F<sub>eq</sub>, F<sub>ap</sub>, and F<sub>br</sub> consist of a double

doublet, a tripletlike double doublet, and a triple triplet, respectively. From the F<sub>eq</sub> and F<sub>br</sub> signals, three coupling constants,  $J_{F_{br}F_{eq}} = 45$  Hz,  $J_{F_{br}F_{ap}} = 22$  Hz, and  $J_{F_{eq}F_{ap}} = 12$  Hz, have been obtained, as summarized in Table IX.<sup>28</sup> The "coupling constant" measured from the tripletlike signal of F<sub>ap</sub> is consistently equal to the averaged coupling constant:  $J_{average} = (J_{F_{br}F_{ap}} + J_{F_{eq}F_{ap}})/2 = 17$  Hz. The symmetrical nature of the fluorine bridge may be attributable to a fast fluorine exchange between pentacoordinate and tetracoordinate silicons with respect to the <sup>19</sup>F NMR time scale, as shown in Scheme IVa, rather than to a "standing" fluorine on the middle point of two silicon atoms, in view of the whole exchange mechanism discussed below. The F<sub>br</sub> exchange is thus the lowest energy process.

**Flipping (b).** The spectrum at -90 °C indicates the presence of two isomers in the ratio of 4:1, on the basis of the peak intensities. These two may be assignable to conformational isomers,<sup>29</sup> F<sub>br</sub>-up and F<sub>br</sub>-down, owing to the flipping of the puckered five-membered ring, as shown in Scheme IVb. The major isomer may be assigned reasonably to the F<sub>br</sub>-up structure, which has been observed in the stable crystals, as determined by X-ray analysis. The F<sub>br</sub>-down isomer might be less stable than the F<sub>br</sub>-up isomer due to the steric repulsion between two phenyl groups in the equatorial position. The flipping is attained by partial rotation about the two endocyclic Si-C bonds, which accompanies the flipping of two equatorial planes. Thus, on the basis of the dihedral angles (71.0 and 66.1°) of these equatorial planes to the central benzene ring observed in the solid state, partial rotation only by (90° - dihedral angle) × 2 = 40–50° should be sufficient for the interconversion of these isomers. At -90 °C, the interconversion may "stop" on the <sup>19</sup>F NMR time scale. When the temperature is increased, the interconversion immediately starts to occur and results in coalescence of each pair at -80 °C. This flipping is thus the next lowest energy process.

**Si-C Rotation (c).** The "Si-C rotation" leads to partial scrambling of fluorine atoms, as shown in Scheme IVc. Rotation about the endocyclic Si-C bonds is possible only after the breaking of one of two F<sub>br</sub>-Si bonds to cause separation into a tetracoordinate and a pentacoordinate silicon moiety. Since there seems to be no large difference in rotational energy barriers between the two Si-C bonds,<sup>31</sup>

(28) Our data are partly consistent with  $J_{F_{br}F_{eq}} = 52$  Hz,  $J_{F_{br}F_{ap}} = 18$  Hz, and  $J_{F_{eq}F_{ap}} = 0$  Hz reported for [(AcO)<sub>2</sub>Si-F<sub>br</sub>-SiF<sub>3</sub>(OAc)]<sup>28</sup> by Brownstein.<sup>12</sup> Holmes has reported  $J_{F_{br}F_{eq}} = 29.6$  Hz for [(TTBP)SiF<sub>4</sub>]<sup>1-</sup>.<sup>6b</sup>

(29) In our preliminary communication,<sup>13</sup> we tentatively assigned the small signals to the trans isomer, but the following analysis has shown those to be assignable to the conformational isomer. If the minor isomer were the trans isomer, there would be two possible mechanisms for cis/trans isomerization of 1. The first involves cleavage of one of the two Si-F<sub>br</sub> bonds followed by full rotation about the Si1-C1 and/or Si2-C2 bond or by pseudorotation of the pentacoordinate silicon moiety, and the other involves isomerization by turnstile rotation<sup>30</sup> of the pentacoordinate silicon species, which proceeds through simultaneous internal rotation of one apical and two equatorial ligands. These two processes, however, must accompany exchange between F<sub>br</sub> and F<sub>ap</sub> and between F<sub>eq</sub> and F<sub>ap</sub>, being inconsistent with the spectral observation that coalescence of the isomer signals around -80 °C does not lead to permutation of F<sub>br</sub>, F<sub>ap</sub>, and F<sub>eq</sub> signals. The possibility for the trans isomer may thus be ruled out.

(30) Ugi, I.; Marquarding, D.; Klusacek, H.; Gillespie, P. *Acc. Chem. Res.* 1971, 4, 288.

(31) Energy barriers for rotation about the Si-C bond have been reported. While only 17.8 cal/mol has been estimated for PhSiH<sub>3</sub>,<sup>31a</sup> 10.9 and 12.9 kcal/mol have been obtained for tris(2,6-xylyl)silane tris(2,6-xylyl)silane and tris(2,6-xylyl)fluorosilane, respectively,<sup>31b,c</sup> indicative of hindered rotation in *ortho*-substituted arylsilanes. The rotational barrier in our cases may thus be comparable to the latter. (a) Caminati, W.; Cazzoli, G.; Mirri, A. M. *Chem. Phys. Lett.* 1975, 31, 475. (b) Boettcher, R. J.; Gust, D.; Mislow, K. *J. Am. Chem. Soc.* 1973, 95, 7157. (c) Hutchings, M. G.; Andose, J. D.; Mislow, K. *J. Am. Chem. Soc.* 1975, 97, 4562.

(27) Relaxation times, T<sub>1</sub> values, of F<sub>br</sub>, F<sub>ap</sub>, and F<sub>eq</sub> in bis(silicate) 1 were measured at -85 °C in acetone-d<sub>6</sub> to be 0.13, 0.31, and 0.27 s, respectively, while T<sub>1</sub> values of F<sub>ap</sub> and F<sub>eq</sub> in [Ph<sub>2</sub>SiF<sub>3</sub>]<sup>-</sup> were 0.45 and 0.48 s, respectively. Thus, T<sub>1</sub> of the bridging fluorine atom F<sub>br</sub> is the smallest of those of all fluorine ligands in bis(silicate), which are smaller than those of mono(silicate).

rotations about two Si-C bonds may occur simultaneously to keep the *cis* configuration favorable for the F<sup>-</sup>...K<sup>+</sup> interactions. The resulting structure should be *degenerate* with the original structure, because two phenyl groups may remain in equatorial positions. Inspection of the column matrix associated with each structure (Scheme IVc), however, indicates that while both apical fluorines change environment, only one of the two equatorial fluorines changes environment: the equatorial fluorine (marked by open arrows) on the pentacoordinate silicon atom remains in the equatorial position. The permutation rate of equatorial fluorines would thus be half of that of apical fluorines.<sup>32</sup> A combination of the F<sub>br</sub>-exchange and Si-C rotation processes results in the degenerate permutation on both silicon sides. The above analysis is consistent with the observed unsymmetrical collapse of the F<sub>ap</sub> and F<sub>eq</sub> resonance in the temperature range from -65 to -33 °C in Figure 8.

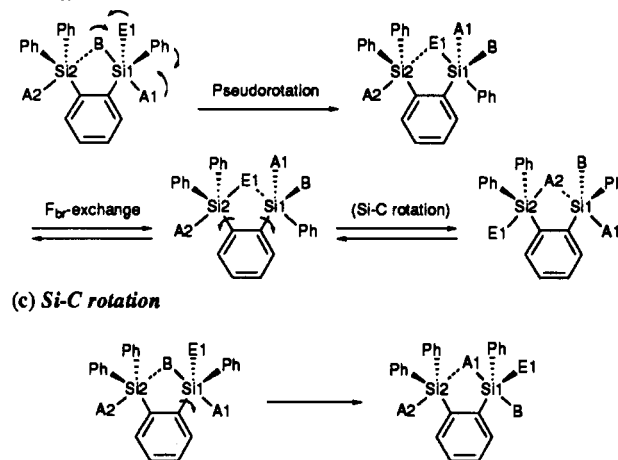
**Pseudorotation (d).** The simultaneous scrambling of all F<sub>eq</sub> and F<sub>ap</sub> atoms can be attained only by a Berry pseudorotation, as shown in Scheme IVd. The resulting isomer 1b, however, should be of higher energy because of the apical phenyl group and hence should undergo rearrangement to a stable isomer such as 1d via the F<sub>br</sub> exchange, partial Si-C rotation, etc. of lower energy; structure 1d is degenerate with the original structure 1a. The pseudorotation, together with three lower energy processes, causes exchange of all five fluorine atoms, to afford coalescence of all resonances. This has been observed around -16 °C, as shown in Figure 8. It has been reported that energy barriers for pseudorotation of mono(siliconates) of the type [ArAr'SiF<sub>3</sub>]<sup>-</sup> are 9-14 kcal/mol, coalescence being observed usually around -20 °C or so.<sup>4,6,15</sup> The ease of pseudorotation in bis(siliconate) 1 seems to be comparable to that of these typical mono(siliconates).

In summary, the fluorine exchange in 1 can be consistently explained by four consecutive processes, in increasing order of energy barriers: (a) F<sub>br</sub> exchange < (b) flipping < (c) Si-C rotation < (d) pseudorotation.

**[F{F}F<sub>2</sub>]<sup>-</sup> (3).** The variable-temperature <sup>19</sup>F NMR spectra of 3 are shown in Figure 10. At -93 °C, four distinct signals appear at -70.40 ppm (broad, F<sub>br</sub>), -108.49 ppm (broad, F<sub>ap1</sub>), -126.62 ppm (s, F<sub>ap2</sub>), and -136.15 ppm (s, F<sub>eq1</sub>), the full data being listed in Table IX. No signal due to a conformational isomer appears, possibly because of the nearly planar F<sub>br</sub>-containing five-membered ring, as determined by X-ray analysis. The assignment of fluorine atoms is based on spectral similarity with other bis(siliconates) and the following variable-temperature data. Two signals due to F<sub>br</sub> and F<sub>ap1</sub> coalesce at -65 °C, and then at -30 °C one broad signal appears at -89.9 ppm, while F<sub>ap2</sub> and F<sub>eq1</sub> signals remain sharp in the range of -93 °C to about -30 °C. Upon continued warming, all peaks broaden at +7 °C and finally a broad singlet appears at -111.4 ppm around +45 °C.

This sequential change may also involve several fluorine ligand exchange processes, as shown in Scheme V. In contrast to the case for 1, there is no need for consideration of flipping (b) of the planar five-membered ring. The exchange mechanisms will be discussed in the order of increasing energy.

(32) It may be noted that this exchange pattern is similar to that observed by <sup>1</sup>H NMR spectroscopy for cyclopentadienylmetal derivatives which undergo 1,2-metallotropy: Bennett, M. J.; Cotton, F. A.; Davison, A.; Faller, J. W.; Lippard, S. J.; Morehouse, S. M. *J. Am. Chem. Soc.* 1966, 88, 4371.

Scheme V<sup>a</sup>(a) F<sub>br</sub>-exchange and (d) Pseudorotation

(c) Si-C rotation

<sup>a</sup> F<sub>br</sub>, F<sub>ap</sub>, and F<sub>eq</sub> are abbreviated B, A, and E, respectively, for clarity.

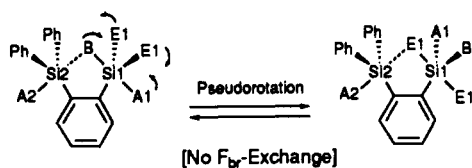
**Si-C Rotation (c).** The first, lowest energy process observed at low temperatures in the range of -93 to -30 °C may be rotation about the Si-C bonds, since the rotation may cause exchange between two fluorines F<sub>br</sub> and F<sub>ap1</sub>, as shown in Scheme Vc, accounting for the coalescence of these two signals only. During the rotational process, the equatorial fluorine (F<sub>eq1</sub>) on Si1 remains in an equatorial position and the Si2 part, which contains only one fluorine atom (F<sub>ap2</sub>), remains as if no rotation has occurred, to keep the fluorine atom in the favorable apical position of TBP geometry. The energy barrier for the rotation about the Si-C bond at the Si1 part can be estimated from the coalescence temperature (-65 °C) to be 8.2 kcal/mol. This is the first estimation of the rotational barrier about the aryl-silicon bond in pentacoordinate siliconates; the data, however, must be considered specific to this bis(siliconate).<sup>31</sup>

**F<sub>br</sub> Exchange (a) and Pseudorotation (d).** The fluorine bridge is unsymmetrical: F<sub>br</sub> is localized on Si1 and interacts weakly with Si2. This situation must be maintained throughout the above Si-C-rotation process, which occurs via cleavage of the weak Si2-F<sub>br</sub> interaction. F<sub>br</sub> exchange thus hardly occurs up to -30 °C. Transfer of F<sub>br</sub> to Si2 followed by Si-C rotation at the Si2 site should be the only process for permutation of F<sub>ap2</sub>, as shown in Scheme Va,d. The F<sub>br</sub> exchange becomes appreciable only at temperatures higher than 7 °C. Around this temperature, pseudorotation at the Si1 site also becomes appreciable simultaneously, resulting in coalescence of all four fluorines (Figure 10). It should be noted that pseudorotation of the pentacoordinated Si2 moiety may not be observed, since the Si2 part is regarded as a nonfluxional [Ar<sub>3</sub>SiF<sub>2</sub>]<sup>-</sup> type.<sup>4a</sup> Another interesting point is that although Si2 in 3 and the two Si groups in 1 are regarded as siliconates of the [Ar<sub>2</sub>SiF<sub>3</sub>]<sup>-</sup> type, the energy barrier for pseudorotation seems to be higher in the former than in the latter. This may be ascribed primarily to the larger steric hindrance by the *o*-FPh<sub>2</sub>Si group in 3 in comparison with the smaller *o*-F<sub>2</sub>PhSi group in 1, in light of the Holmes observations.<sup>6</sup>

**[F{F}F<sub>3</sub>]<sup>-</sup> (2).** The variable-temperature <sup>19</sup>F NMR spectra are presented in Figure 11. As listed in Table IX, at -110 °C in THF-*d*<sub>3</sub>, four fluorine signals are observed at -77.53 ppm (1 F), -118.89 ppm (1 F), -130.51 ppm (1 F), and -134.77 ppm (2 F), assignable to F<sub>br</sub>, F<sub>ap1</sub>, F<sub>ap2</sub>, and two F<sub>eq1</sub> atoms, respectively, in light of the assignment for

Scheme VI<sup>a</sup>

(d) Pseudorotation



<sup>a</sup>  $F_{br}$ ,  $F_{ap}$ , and  $F_{eq}$  are abbreviated B, A, and E, respectively, for clarity.

1 and 3. It should be noted here that neither a stereoisomer nor a conformational isomer is present in 2. As the temperature increases, the three fluorine signals ( $F_{br}$ ,  $F_{ap1}$ , and  $2 \times F_{eq1}$ ) due to four fluorine atoms all on Si1 broaden and at  $-90^\circ\text{C}$  coalesce into a new signal at  $-117$  ppm, while the remaining sharp singlet ( $F_{ap2}$ ) moves slightly to upper field. Finally, at  $+22^\circ\text{C}$ , two sharp signals appear at  $-117$  ppm (4 F) and  $-137$  ppm (1 F) due to the  $-\text{SiF}_4^-$  and  $-\text{SiPh}_2\text{F}$  group, respectively. Upon continued warming in DMSO- $d_6$ , only the broadening of the two singlet peaks was observed up to  $+90^\circ\text{C}$ ; further heating led to decomposition of 2. The results reveal that at temperatures higher than room temperature the two silyl groups in 2 exist as an anionic silicate of  $[\text{ArSiF}_4]^-$  type and the neutral silane  $\text{ArSiPh}_2\text{F}$ .

The ligand-exchange processes may be explained only by pseudorotation (d) at the Si1 site, as shown in Scheme VI. This is the lowest energy process, detectable only below  $-90^\circ\text{C}$ . The Si-C rotation (c) should occur in the next step, at higher than  $-90^\circ\text{C}$  in view of the energy barrier estimated for 3, but would be hidden by the pseudorotation process. Worthy of note is that  $F_{br}$  exchange (a) has never been observed in 2 and must be the highest energy process, in sharp contrast to the case for 1. The flipping process (b) is not detectable experimentally in this case, since both silicon centers are not chiral. Finally, it should be mentioned that the Si1 side in 2 is the second example of  $[\text{ArSiF}_4]^-$  type silicates where the pseudorotation has been observed by  $^{19}\text{F}$  NMR spectroscopy; the first is Holmes'  $[(\text{TBP})\text{SiF}_4]^-$ .<sup>6b</sup>

In summarizing the above results, we will attempt to correlate the ligand-exchange processes with the structural aspects of bis(siliconates) determined by X-ray analysis. The relative ease of the ligand-exchange processes, the pentacoordination character (% TBP) of each silicon atom, and the difference in % TBP between Si1 and Si2,  $\Delta(\% \text{TBP})$ , are listed in Table V in the order of an increase in  $\Delta(\% \text{TBP})$ . There are several significant features. (1) Flipping (b) has been observed only in 1. (2) The energy barrier of  $F_{br}$  exchange (a) increases in the order  $1 < 3 < 2$ , being parallel with the order of an increase in  $\Delta(\% \text{TBP})$ . Thus,  $F_{br}$  exchange, which is the lowest energy process in 1, becomes the highest energy process in 2. In other words, while in bis(siliconates) 1 and 3, whose  $\Delta(\% \text{TBP})$  is smaller than 20%, the fluoride exchange between penta- and tetracoordinate silicon atoms is much faster than  $^{19}\text{F}$  NMR time scale, in the highly unsymmetrical bis(siliconate) 2, whose  $\Delta(\% \text{TBP})$  is larger than 40%,  $F_{br}$  exchange is too slow to detect by  $^{19}\text{F}$  NMR spectroscopy. It should be noted that the  $F_{br}$  exchange is comparable with or faster than the  $^{13}\text{C}$  NMR time scale, as discussed above.<sup>25</sup> (3) Energy barriers of Si-C rotation (c) in 1-3 seem to be comparable with each other. (4) While pseudorotation (d) is the slowest process in 1 and 3, which contain a  $[\text{Ar}_2\text{SiF}_4]^-$  type silicate, pseudorotation is the fastest, lowest energy process in 2, which has a  $[\text{ArSiF}_4]^-$  type silicate. As a result, the relative ease of processes

Table X. Correlation between Intramolecular Ligand-Exchange Processes  $F_{br}$  Exchange (a), Flipping (b), Si-C Rotation (c), and Pseudorotation (d) and Pentacoordination Character of Bis(siliconates)

bis(siliconate)	rel order of energy barriers	pentacoordination character (% TBP) <sup>a</sup>	
		Si2, Si1	$\Delta(\% \text{TBP})^b$
$[\text{F}_2\{\text{F}\}\text{F}_2]^-$ (anion of 1)	$a < b < c < d$	66, 78	12
$[\text{F}\{\text{F}\}\text{F}_2]^-$ (anion of 3) <sup>c</sup>	$c < a \approx d$	68, 88	20
$[\text{F}\{\text{F}\}\text{F}_3]^-$ (anion of 2) <sup>c</sup>	$d < c \ll a$	50, 93	43

<sup>a</sup> Estimated from X-ray structures. <sup>b</sup>  $\Delta(\% \text{TBP}) = |(\% \text{TBP}_a \text{ of Si1}) - (\% \text{TBP}_a \text{ of Si2})|$ . <sup>c</sup> Flipping process b is not present.

a, c, and d in 2 is the reverse of that in 1, as shown in Table X.

In this study, we have shown that three new mechanisms operate in intramolecular ligand-exchange processes in bis(siliconates), in addition to the traditional "pseudorotation" observed in mono(siliconates). It has also been demonstrated that the fluxional behavior of bis(siliconates) in solution can be closely correlated with the solid-state structures determined by X-ray analysis.

### Experimental Section

**General Remarks.**  $^1\text{H}$ ,  $^{19}\text{F}$ , and  $^{29}\text{Si}$  NMR spectra were recorded on a Varian VXR-200 spectrometer, operated at 200, 188.15, and 39.73 MHz, respectively.  $^{13}\text{C}$  NMR spectra were obtained on a Varian VXR-200 (50.29 MHz) or a JEOL JNM-GX-400 instrument (100.59 MHz).  $^1\text{H}$  and  $^{13}\text{C}$  chemical shifts are referenced to internal acetone- $d_6$  ( $^1\text{H}$ ,  $\delta$  2.05 ppm;  $^{13}\text{C}$ ,  $\delta$  29.8 ppm) or  $\text{CDCl}_3$  ( $^1\text{H}$ ,  $\delta$  7.24 ppm) relative to  $\text{Me}_4\text{Si}$  at 0 ppm.  $^{19}\text{F}$  chemical shifts refer to  $\text{CFCl}_3$  ( $^{19}\text{F}$ ,  $\delta$  0 ppm) as an internal standard.  $^{29}\text{Si}$  chemical shifts are reported relative to  $\text{Me}_4\text{Si}$  in ppm.  $^{29}\text{Si}$  NMR experiments were performed with proton decoupling, using a standard  $^{13}\text{C}$  pulse program.

**Solid-State  $^{29}\text{Si}$  NMR Studies.**  $^{29}\text{Si}$  NMR spectra in the solid state were obtained on a Varian Unity 400 spectrometer at 79.46 MHz. Magic-angle spinning and proton-gated decoupling were employed. Samples were introduced into a 5-mm NMR tube and spun at 4-5 kHz. The pulse delay was 100-200 s. Spectra were recorded at  $25^\circ\text{C}$ . The 4,4-dimethyl-4-silapentanesulfonic acid sodium salt (DSS;  $\delta$  0 ppm) was used as the external standard.

**Variable-Temperature  $^{19}\text{F}$  NMR Studies.** Variable-temperature experiments were carried out in acetone- $d_6$  and THF- $d_6$  with temperature calibration accomplished by using a standard methanol sample. The calibration error was  $\pm 1.0^\circ\text{C}$ .

**X-ray Studies.** All crystals used for the X-ray studies were recrystallized from acetone to give the colorless crystals. Intensity data were collected at  $23^\circ\text{C}$  on a Rigaku AFC-5R diffractometer using graphite-monochromatized  $\text{Cu K}\alpha$  radiation ( $\lambda = 1.54178 \text{ \AA}$ ) and  $\omega$ - $2\theta$  scan values for 20 reflections in the range  $35^\circ \leq 2\theta \leq 40^\circ$ . No significant changes in the intensities of 3 standard reflections monitored every 100 measurements were observed during data collection. The structures were solved by use of the program MULTAN87<sup>33</sup> and refined by the block-diagonal least-squares method to minimize the function  $\sum(w|\Delta F|^2)$ . Corrections for absorption were applied after isotropic least-squares refinement for the non-H atoms, by an empirical method based on the differences between the observed and calculated structure factors.<sup>34</sup> Many of the H atoms were located in a difference electron density map, the others being stereochemically positioned. Positional parameters of all the atoms and anisotropic thermal parameters of the non-H atoms were refined: the temperature factor of each H atom was assumed to be isotropic and estimated to be equal to the equivalent isotropic temperature factor of the bonded atom.

(33) Debaerdemaeker, T.; Germain, G.; Main, P.; Tate, C.; Woolfson, M. M. MULTAN87 Computer Programs for the Automatic Solution of Crystal Structures from X-ray Diffraction Data; University of York: York, England, 1987.

(34) Walker, N.; Stuart, D. *Acta Crystallogr.* 1983, A39, 158.

Atomic scattering factors were calculated by the analytical approximation  $\sum [a_i \exp(-b_i(\sin^2 \theta)/\lambda^2)] + c$  ( $i = 1-4$ ).<sup>35</sup> All computations were performed on a FACOM M-340R computer at Shionogi Research Laboratories. No handedness of 1 and 2 has been determined because differences in the  $R$  values respectively calculated on the basis of the right- and left-handed atomic coordinate systems were not significant. Crystallographic details are listed in Table IV. Bond lengths for the 18-crown-6 parts of all the compounds, in which the atoms are subjected to thermal motions with large anisotropy, are shorter than the corresponding normal values.

**Materials.** Hexane, tetrahydrofuran (THF), and toluene were distilled from lithium aluminum hydride and stored under nitrogen, while dichloromethane and 2-propanol were purified by distillation from calcium hydride under nitrogen and kept over 4-Å molecular sieves activated by heating to 250 °C for 5 h and cooling in vacuo. *tert*-Butyllithium in pentane was purchased from Kanto Chemical Co., Inc. Spray-dried KF was commercially available from Wako Pure Chemical Industry. Tetrafluoroboric acid-diethyl ether complex (85%) was obtained from Aldrich Chemical Co., Inc.

**Diphenylbis(*N,N,N'*-trimethylethylenediamino)silane (4).** To a solution of *N,N,N'*-trimethylethylenediamine (10.98 g, 107.5 mmol) in dry THF (65 mL) was added dropwise *n*-butyllithium (1.6 M in hexane; 67.2 mL, 107.5 mmol) over 30 min at 0 °C under nitrogen, and the reaction mixture was stirred at 0 °C for 2 h. Diphenyldichlorosilane (8.77 mL, 42.3 mmol) was added dropwise to this solution over 10 min at 0 °C. After the addition was complete, the reaction mixture was warmed to room temperature and stirred for 12 h. Filtration through Celite and evaporation of solvents gave a tarry oil. This residue was diluted with hexane (100 mL) in order to ensure precipitation of insoluble salts. The mixture was filtered through Celite and distilled after evaporation of solvents to give 14.28 g (88% yield) of diaminodiphenylsilane 4: bp 174–176 (0.5 mmHg); <sup>1</sup>H NMR (C<sub>6</sub>D<sub>6</sub>) δ 2.084 (s, 12 H), 2.425 (t,  $J = 7.4$  Hz, 4 H), 2.736 (s, 6 H), 3.127 (t,  $J = 7.4$  Hz, 4 H), 7.245–7.357 (m, 6 H), 7.796–7.878 (m, 4 H). Anal. Calcd for C<sub>22</sub>H<sub>38</sub>N<sub>4</sub>Si: C, 68.70; H, 9.43. Found: C, 68.90; H, 9.61.

**Phenyltris(*N,N,N'*-trimethylethylenediamino)silane (7).** In a similar manner, *N,N,N'*-trimethylethylenediamine (12.64 g, 123.7 mmol), *n*-butyllithium (1.6 M in hexane; 77.3 mL, 123.7 mmol), and phenyltrichlorosilane (5.6 mL, 35.3 mmol) gave 11.87 g (76% yield) of phenyltriaminosilane 7: bp 151–153 °C (0.2 mmHg); <sup>1</sup>H NMR (C<sub>6</sub>D<sub>6</sub>) δ 2.162 (s, 18 H), 2.453 (t,  $J = 7.5$  Hz, 6 H), 2.695 (s, 9 H), 3.105 (t,  $J = 7.5$  Hz, 6 H), 7.247–7.376 (m, 3 H), 7.803–7.891 (m, 2 H). Anal. Calcd for C<sub>24</sub>H<sub>44</sub>N<sub>6</sub>Si: C, 61.71; H, 10.85. Found: C, 61.51; H, 10.92.

**1,3-Diisopropoxy-1,3-diphenyl-2-oxa-1,3-disilaindan (5).** To diphenyldiaminosilane 4 (1.91 g; 5.3 mmol) was added a pentane solution of *t*-BuLi (1.4 M; 8.6 mL, 12.0 mmol) at 0 °C under nitrogen. The mixture was stirred at 0 °C for 1 h and at room temperature for another 1 h. Phenyltrichlorosilane (6.45 mL, 40.5 mmol) was added to the mixture at 0 °C, and the mixture was heated at 50 °C for 3 h. To the resulting mixture was added 2-propanol (10 mL) at room temperature, followed by stirring for 12 h, and then Et<sub>3</sub>N (7.5 mL, slightly exothermic) and water (95 μL, 5.3 mmol) were successively added. After filtration, the filtrate was dried over MgSO<sub>4</sub>, evaporated, and then distilled to remove volatile phenyltriisopropoxysilane. The residue was subjected to column chromatography on silica gel (hexane–EtOAc, 20:1;  $R_f$  0.42) to give 5 in 57% yield as a *cis/trans* mixture (purity >95% by GLC and NMR): <sup>1</sup>H NMR (CDCl<sub>3</sub>) δ 1.113 (d,  $J = 6.2$  Hz), 1.151 (d,  $J = 6.2$  Hz), 1.233 (d,  $J = 6.0$  Hz), 1.301 (d,  $J = 6.2$  Hz) (total 12 H), 4.087 (septet,  $J = 6.1$  Hz), 4.277 (septet,  $J = 6.1$  Hz) (total 2 H), 7.277–7.501 (m), 7.635–7.801 (m) (total 14 H); IR (liquid film, cm<sup>-1</sup>) 2984 (s), 1122 (vs), 1038 (s), 832 (vs), 732 (s), 714 (s), 700 (s); MS  $m/z$  421 (M<sup>+</sup> + 1, 28), 420 (M<sup>+</sup>, 76), 377 (61), 342 (85), 118 (100). Anal. Calcd for C<sub>24</sub>H<sub>28</sub>O<sub>3</sub>Si<sub>2</sub>: C, 68.53; H, 6.71. Found: C, 68.69; H, 6.82.

**1,1-Diisopropoxy-3,3-diphenyl-2-oxa-1,3-disilaindan (8).** To phenyltriaminosilane 7 (2.94 g, 7.2 mmol) was added *t*-BuLi (1.4 M in pentane; 12.3 mL, 17.3 mmol) at –20 °C under nitrogen. The

mixture was stirred at –20 °C for 1 h and at room temperature for 2 h. Diphenyldichlorosilane (11.9 mL, 57.4 mmol) was added to the mixture at 0 °C, and the mixture was heated at 50 °C for 3 h. To the resulting mixture was added 2-propanol (12 mL) at 0 °C, followed by stirring at room temperature for 12 h, and then Et<sub>3</sub>N (11.5 mL, slightly exothermic) and water (128 μL, 7.2 mmol) were successively added. After filtration, the filtrate was dried over MgSO<sub>4</sub>, evaporated, and then distilled to remove volatile diphenyldiisopropoxysilane. The residue was subjected to column chromatography on silica gel (hexane–EtOAc, 20:1;  $R_f$  0.27) gave 8 in 27% yield (purity ca. 95% by GLC and NMR; the analytical sample was further purified by preparative GLC). <sup>1</sup>H NMR (CDCl<sub>3</sub>) δ 1.104 (d,  $J = 6.2$  Hz, 6 H), 1.163 (d,  $J = 6.0$  Hz, 6 H), 4.138 (septet,  $J = 6.1$  Hz, 2 H), 7.286–7.534 (m, 8 H), 7.630–7.811 (m, 6 H); IR (liquid film, cm<sup>-1</sup>) 2980 (s), 1432 (s), 1122 (vs), 1044 (vs), 930 (vs), 736 (s), 716 (s), 700 (s); MS  $m/z$  420 (M<sup>+</sup>, 2.4), 405 (7), 342 (100). Anal. Calcd for C<sub>24</sub>H<sub>28</sub>O<sub>3</sub>Si<sub>2</sub>: C, 68.53; H, 6.71. Found: C, 68.26; H, 6.71.

**1-Isopropoxy-1,3,3-triphenyl-2-oxa-1,3-disilaindan (10).** To diphenyldiaminosilane 4 (2.73 g, 7.1 mmol) was added *t*-BuLi (1.4 M in pentane; 12.2 mL, 17.0 mmol) at –30 °C under nitrogen. The mixture was stirred at –30 °C for 1 h and at room temperature for 2 h. Diphenyldichlorosilane (11.8 mL, 56.8 mmol) was added to the mixture at 0 °C, and the mixture was stirred at room temperature for 1 h and heated at 50 °C for 2 h. To the resulting mixture was added 2-propanol (8 mL) at 0 °C, followed by stirring at room temperature for 12 h and addition of Et<sub>3</sub>N (11 mL). After filtration, the filtrate was evaporated and distilled to remove volatile diphenyldiisopropoxysilane. The residue was subjected to column chromatography on silica gel (hexane–EtOAc, 20:1;  $R_f$  0.20) to give 10 in 77% yield (purity >95% by GLC and NMR): <sup>1</sup>H NMR (CDCl<sub>3</sub>) δ 1.109 (d,  $J = 6.0$  Hz, 3 H), 1.133 (d,  $J = 6.0$  Hz, 3 H), 4.089 (septet,  $J = 6.0$  Hz, 1 H), 7.258–7.826 (m, 19 H); IR (liquid film, cm<sup>-1</sup>) 3056 (s), 2980 (s), 1432 (s), 1384 (s), 1372 (s), 1124 (vs), 1038 (vs), 924 (vs), 792 (s), 734 (s), 712 (s), 700 (s); MS  $m/z$  438 (M<sup>+</sup>, 5), 360 (100); HRMS calcd for C<sub>27</sub>H<sub>26</sub>O<sub>2</sub>Si<sub>2</sub> 438.1470, found 438.1462.

***o*-Bis(difluorophenylsilyl)benzene (6).** To a solution of 5 (414 mg, 1.0 mmol) in CH<sub>2</sub>Cl<sub>2</sub> was added HBF<sub>4</sub>·OEt<sub>2</sub> (981 mg, 6.1 mmol) at 0 °C under nitrogen. After it was stirred at 0 °C for 12 h, the mixture was bulb-to-bulb-distilled to give 6 in 88% yield (purity >95% by GLC and <sup>19</sup>F NMR): bp 207–211 °C (1.6 mmHg); <sup>1</sup>H NMR (acetone-*d*<sub>6</sub>) δ 7.42–8.06 (m); <sup>13</sup>C NMR (acetone-*d*<sub>6</sub>, 50.29 MHz) δ 129.27, 132.55, 133.19, 135.10, 137.52 (Si ipso carbons are hidden in the 129.27 signal); <sup>19</sup>F NMR (acetone-*d*<sub>6</sub>) δ –137.68 (<sup>1</sup> $J_{\text{FSi}}$  = 292.96 Hz); <sup>29</sup>Si NMR (acetone-*d*<sub>6</sub>) δ –30.21 (t, <sup>1</sup> $J_{\text{SiF}}$  = 293.92 Hz); MS  $m/z$  363 (M<sup>+</sup> + 1, 30), 362 (M<sup>+</sup>, 100), 219 (81), 91 (51); HRMS calcd for C<sub>18</sub>H<sub>14</sub>F<sub>4</sub>Si<sub>2</sub> 362.0570, found 362.0565.

***o*-(Fluorodiphenylsilyl)(trifluorosilyl)benzene (9).** To a solution of 8 (545 mg, 1.3 mmol) in CH<sub>2</sub>Cl<sub>2</sub> was added HBF<sub>4</sub>·OEt<sub>2</sub> (1.319 g, 8.1 mmol) at 0 °C under nitrogen. After it was stirred at 0 °C for 12 h, the mixture was bulb-to-bulb-distilled to give 9 in 72% yield (purity >95% by GLC and <sup>19</sup>F NMR): bp 196–201 °C (1.5 mmHg); <sup>1</sup>H NMR (acetone-*d*<sub>6</sub>) δ 7.380–7.825 (m, 13 H), 8.025–8.153 (m, 1 H); <sup>19</sup>F NMR (acetone-*d*<sub>6</sub>) δ –138.16 (d, <sup>5</sup> $J_{\text{FF}}$  = 16.56 Hz, <sup>1</sup> $J_{\text{FSi}}$  = 266.04 Hz, 3 F), –164.19 (q, <sup>5</sup> $J_{\text{FF}}$  = 15.37 Hz, 1 F); <sup>29</sup>Si NMR (acetone-*d*<sub>6</sub>) δ –3.63 (d, <sup>1</sup> $J_{\text{SiF}}$  = 282.08 Hz), –73.46 (q, <sup>1</sup> $J_{\text{SiF}}$  = 265.42 Hz); IR (liquid film, cm<sup>-1</sup>) 1434 (s), 1142 (s), 1126 (s), 950 (vs), 854 (vs), 738 (s), 718 (s), 700 (s); MS  $m/z$  363 (M<sup>+</sup> + 1, 14), 362 (M<sup>+</sup>, 49), 340 (77) 201 (100), 154 (60); HRMS calcd for C<sub>18</sub>H<sub>14</sub>F<sub>4</sub>Si<sub>2</sub> 362.0570, found 362.0580.

***o*-(Difluorophenylsilyl)(fluorodiphenylsilyl)benzene (11).** To a solution of 10 (564 mg, 1.3 mmol) in CH<sub>2</sub>Cl<sub>2</sub> (7 mL) was added HBF<sub>4</sub>·OEt<sub>2</sub> (1.208 g, 7.5 mmol) at 0 °C under nitrogen. After it was stirred at 0 °C for 12 h, the mixture was bulb-to-bulb-distilled to give 11 in 87% yield (purity ca. 90% by GLC and <sup>19</sup>F NMR): bp 259–265 °C (1.5 mmHg); <sup>1</sup>H NMR (200 MHz, acetone-*d*<sub>6</sub>) δ 7.360–7.622 (m, 14 H), 7.638–7.792 (m, 4 H), 8.024–8.087 (m, 1 H); <sup>19</sup>F NMR (188.15 MHz, acetone-*d*<sub>6</sub>) δ –137.86 (d, <sup>5</sup> $J_{\text{FF}}$  = 13.73 Hz, <sup>1</sup> $J_{\text{FSi}}$  = 292.95 Hz, 2 F), –160.68 (t, <sup>5</sup> $J_{\text{FF}}$  = 13.73 Hz, <sup>1</sup> $J_{\text{FSi}}$  = 284.67 Hz, 1 F); <sup>29</sup>Si NMR (39.73 MHz, acetone-*d*<sub>6</sub>) δ –3.51 (d, <sup>1</sup> $J_{\text{SiF}}$  = 284.1 Hz), –30.14 (t, <sup>1</sup> $J_{\text{SiF}}$  = 292.4 Hz); IR (liquid film, cm<sup>-1</sup>) 1434 (s), 1126 (vs), 908 (vs), 850 (vs), 752 (s), 742 (s), 698 (s); MS  $m/z$  421 (M<sup>+</sup> + 1, 23), 420 (M<sup>+</sup>, 64), 343 (100), 266 (32); HRMS calcd for C<sub>24</sub>H<sub>10</sub>F<sub>3</sub>Si<sub>2</sub> 420.0977, found

(35) Cromer, D. T.; Waber, J. T. *International Tables for X-ray Crystallography*; Kynoch Press: Birmingham, England, 1973; Vol. IV, Table 2.2B.

420.0992.

**Potassium 18-Crown-6 ( $\mu$ -Fluoro)( $\mu$ -1,2-benzenediyl)-*Si,Si,Si',Si'*-tetrafluoro-*Si,Si'*-diphenylbis(siliconate), [*o*-C<sub>6</sub>H<sub>4</sub>(SiPhF<sub>2</sub>)<sub>2</sub>F]<sup>-</sup>,K<sup>+</sup>18-crown-6 (1).** Treatment of *o*-bis(difluorophenylsilyl)benzene (6; 384 mg, 1.1 mmol) with spray-dried KF (68 mg, 1.1 mmol) and 18-crown-6 (308 mg, 1.1 mmol) in dry toluene (2.5 mL) at room temperature for 20 h gave white crystalline solids. The solids were filtered in air and washed with ether (30 mL). The remaining solids were treated with ca. 10 mL of THF, heated at reflux, and filtered hot to remove excess KF. Upon cooling of the filtrate, fine crystals deposited. Recrystallization from THF gave pure 1 (462 mg, 64% yield): mp 149.5–150.5 dec; <sup>1</sup>H NMR (acetone-*d*<sub>6</sub>, 200 MHz)  $\delta$  3.554 (s, 24 H), 7.137–7.256 (m, 6 H), 7.409 (dd, *J* = 5.6, 3.4 Hz, 2 H), 7.868–7.951 (m, 4 H), 8.208 (dd, *J* = 5.6, 3.4 Hz, 2 H); <sup>19</sup>F NMR (acetone-*d*<sub>6</sub>, 188.15 MHz; +22 °C)  $\delta$  -117.33 (br); IR (KBr, cm<sup>-1</sup>) 3060 (w), 2908 (m), 1474 (w), 1462 (w), 1436 (m), 1288 (w), 1254 (m), 1112 (s), 966 (m), 836 (m), 748 (m), 714 (m), 552 (m). Anal. Calcd For C<sub>30</sub>H<sub>38</sub>O<sub>6</sub>F<sub>5</sub>Si<sub>2</sub>K: C, 52.61; H, 5.59; F, 13.87. Found: C, 52.35; H, 5.55; F, 14.06.

**Potassium 18-Crown-6 ( $\mu$ -Fluoro)( $\mu$ -1,2-benzenediyl)-*Si,Si,Si,Si'*-tetrafluoro-*Si,Si'*-diphenylbis(siliconate), [*o*-C<sub>6</sub>H<sub>4</sub>(SiF<sub>3</sub>)(SiPh<sub>2</sub>F)F]<sup>-</sup>,K<sup>+</sup>18-crown-6 (2).** Treatment of *o*-(fluorodiphenylsilyl)(trifluorosilyl)benzene (9; 220 mg, 0.61 mmol) with spray-dried KF (36 mg, 0.62 mmol) and 18-crown-6 (168 mg, 0.64 mmol) in dry toluene (2 mL) at room temperature over 1 day gave white crystals. The solids were filtered, washed with ether (30 mL), and recrystallized from dry THF as above to give pure 2 (291 mg, 70% yield): mp 146.5–147.0 °C dec; <sup>1</sup>H NMR (acetone-*d*<sub>6</sub>)  $\delta$  3.638 (s, 24 H), 7.175–7.246 (m, 6 H), 7.336 (broad t, *J* = 6.47 Hz, 1 H), 7.394 (dt, *J* = 7.30, 1.63 Hz, 1 H), 7.816–7.877 (m, 4 H), 8.195 (broad d, *J* = 7.66 Hz, 1 H), 8.217 (ddd, *J* = 7.39, 1.04, 0.65 Hz, 1 H); <sup>19</sup>F NMR (acetone-*d*<sub>6</sub>; +22 °C)  $\delta$  -117.19 (s, <sup>1</sup>*J*<sub>F<sub>Si</sub></sub> = 209.79 Hz, 4 F), -151.03 (s, 1 F); IR (liquid film, cm<sup>-1</sup>) 2892 (m), 2832 (w), 1474 (w), 1456 (w), 1432 (w), 1354 (s), 1256 (w), 1112 (vs), 964 (s), 864 (m), 842 (w), 790 (s), 758 (w), 742 (m), 730 (m), 700 (s), 540 (m), 498 (m), 484 (m). Anal. Calcd for C<sub>30</sub>H<sub>38</sub>O<sub>6</sub>F<sub>5</sub>Si<sub>2</sub>K: C, 52.61; H, 5.59; F, 13.87. Found: 52.36; H,

5.60; F, 14.02.

**Potassium 18-Crown-6 ( $\mu$ -Fluoro)( $\mu$ -1,2-benzenediyl)-*Si,Si,Si'*-trifluoro-*Si,Si',Si'*-triphenylbis(siliconate), [*o*-C<sub>6</sub>H<sub>4</sub>(SiPhF<sub>2</sub>)(SiPh<sub>2</sub>F)F]<sup>-</sup>,K<sup>+</sup>18-crown-6 (3).** Treatment of *o*-(difluorophenylsilyl)(fluorodiphenylsilyl)benzene (11; 440 mg, 1.1 mmol), purified by preparative GLC, with spray-dried KF (63 mg, 1.1 mmol) and 18-crown-6 (296 mg, 1.1 mmol) in dry toluene (2 mL) at room temperature over 2 days gave white crystals. The solids were filtered, washed with ether (30 mL), and recrystallized from dry THF to give pure 3 (444 mg, 57% yield): mp 153.5–155.0 °C dec; <sup>1</sup>H NMR (acetone-*d*<sub>6</sub>)  $\delta$  3.603 (s, 24 H), 6.867–7.248 (m, 8 H), 7.273–7.419 (m, 3 H), 7.440–7.540 (m, 2 H), 7.764–7.874 (m, 4 H), 8.253–8.356 (m, 2 H); <sup>19</sup>F NMR (acetone-*d*<sub>6</sub>) +20 °C no signal, +45 °C -111.4 (br); IR (KBr, cm<sup>-1</sup>) 3048 (w), 2896 (m), 2828 (w), 1476 (w), 1456 (w), 1432 (m), 1354 (s), 1286 (w), 1250 (m), 1108 (s), 964 (s), 838 (m), 802 (s), 742 (s), 704 (s), 660 (s), 554 (s), 528 (m), 514 (s), 498 (m). Anal. Calcd for C<sub>36</sub>H<sub>48</sub>O<sub>6</sub>F<sub>4</sub>Si<sub>2</sub>K: C, 58.20; H, 5.38; F, 10.23. Found: C, 58.12; H, 5.85; F, 10.31.

**Acknowledgment.** We acknowledge the Ministry of Education, Science, and Culture of Japan for Grants-in-Aid for Scientific Research on Priority Area of Organic Unusual Valency (Nos. 02247103 and 03233104). We thank Professor Robert R. Holmes of the University of Massachusetts at Amherst for valuable suggestions and fruitful discussion and Mr. Haruo Fujita of our department and Mr. Katsuhiko Kushida of Varian Instruments Ltd. for measurements of 100-MHz <sup>13</sup>C NMR and solid-state <sup>29</sup>Si NMR spectra, respectively. Thanks are also due to Shin-etsu Chemical Co., Ltd., for a gift of phenylchlorosilanes.

**Supplementary Material Available:** Tables S-I-S-XII, listing atomic coordinates, thermal parameters, and all bond lengths and angles for 1–3 (15 pages). Ordering information is given on any current masthead page.

OM9200518